Available online at www.sciencedirect.com
ScienceDirect
Journal of Power Sources 165 (2007) 455–480
JOURNAL OF POWER SOURCES
www.elsevier.com/locate/jpowsour

Review

The development of a micropower (micro-thermophotovoltaic) device

Loy Chuan Chia, Bo Feng *

School of Engineering, The University of Queensland, St. Lucia, Qld. 4072, Australia

Received 31 July 2006; received in revised form 3 December 2006; accepted 5 December 2006
Available online 16 January 2007

Abstract

A detailed review is carried out on current micropower technology. In particular, a prototype micropower device based on the concept of a thermophotovoltaic (TPV) system of generating electricity is reviewed in this report. This prototype micro-TPV power generator [W.M. Yang, S.K. Chou, C. Shu, H. Xue, Z.W. Li, J. Phys. D: Appl. Phys. 37 (2004) 1017–1020] is currently under research and development by the National University of Singapore (NUS). Focus is made on the possible improvements to the micro-TPV power device, in particular the efficiency of the micro-combustor, PV cells, and consequently the overall the efficiency.

Keywords: Micropower device; Micro-combustion; Thermophotovoltaic; Micro-combustor

Contents

1. Introduction 456
   1.1. Motivation 456
   1.2. Significance and need for micropower device 456
   1.3. Current situation (batteries) 457
   1.4. Potential solutions for micropower generation 457
      1.4.1. Hydrocarbon fuel 457
      1.4.2. Power MEMS 458
   1.5. Summary of micropower technology 458
   1.6. Outline of this review 458
2. Approaches to micropower generation 458
   2.1. Types and examples of micropower generation devices 458
      2.1.1. Micro-gas turbine engines and micro-rotary engines 459
      2.1.2. Micro-thermoelectric 459
      2.1.3. Micro-fuel cell 459
      2.1.4. Micro-electromagnetic 460
      2.1.5. Micro-thermophotovoltaic (micro-TPV) 460
   2.2. Problems with micro-scale combustion and power generation 460
      2.2.1. Heat loss and quenching 460
      2.2.2. Fabrication and materials 461
   2.3. Summary of micropower approaches 461
3. Introduction to thermophotovoltaic system 461
   3.1. Background 461
   3.2. Principle of thermophotovoltaic (TPV) system 461

* Corresponding author. Tel.: +61 7 3346 9193; fax: +61 7 3365 4799.
E-mail address: b.feng@uq.edu.au (B. Feng).

0378-7753/$ – see front matter © 2006 Elsevier B.V. All rights reserved.
doi:10.1016/j.jpowsour.2006.12.006

3.3. Efficiency of thermophotovoltaic (TPV) system ... 462
3.4. Advantages of thermophotovoltaic (TPV) system ... 462
4. A micro-thermophotovoltaic power device ... 462
4.1. Introduction ... 462
4.2. Design and structure of the micro-TPV power device ... 462
4.3. Operating principles of the micro-TPV power device ... 463
4.4. Components of the micro-TPV power device ... 463
4.4.1. Micro-combustor ... 463
4.4.2. SiC emitter ... 464
4.4.3. Dielectric filter ... 464
4.4.4. Photovoltaic (PV) cell array ... 465
4.4.5. Cooling fins ... 466
4.5. Investigation and experimental studies ... 467
4.5.1. Micro-combustion studies (flow rate and H_2/air ratio) ... 467
4.5.2. Effects of wall thickness of micro-combustor ... 469
4.5.3. Micro-combustor with and without backward facing step ... 471
4.5.4. Effects of step height of the micro-combustor ... 473
4.6. Summary of investigation results ... 474
5. Efficiency improvements for a micro-TPV device ... 474
5.1. Introduction ... 474
5.2. Efficiency of micro-combustor (SiC emitter) and overall efficiency ... 474
5.3. Possible efficiency improvements ... 475
5.3.1. Replacing the material of the PV cells ... 475
5.3.2. Replacing the material of the emitter ... 476
5.3.3. Increasing the length of micro-combustor ... 476
5.3.4. Increasing other physical dimensions of micro-combustor ... 477
5.3.5. Employing a catalytic combustion ... 477
5.3.6. Replacing with Co/Ni-doped MgO emitter and increasing length ... 478
5.4. Summary of the possible efficiency improvements ... 478
6. Conclusions and recommendations ... 478
6.1. Conclusions ... 478
6.2. Future work ... 479
Acknowledgement ... 479
References ... 479

1. Introduction

1.1. Motivation

The development of micropower devices is motivated by the increasing needs and demand for smaller scale and higher density power sources. Traditional batteries have failed to satisfy this need, due to relatively low projected energy densities, thus causing serious logistical mission constraints [1]. Mass and volume have also become important criteria in the growing trend towards the miniaturisation of both mechanical and electromechanical engineering devices. All kinds of micro-devices are being developed rapidly. This need for a tiny but powerful energy source is urgent. A micro-scale power system had been strongly regarded as a viable solution and an alternative power source. The micropower concept is still relatively new, as such, and not many micropower devices have been developed. By doing a detailed review of the currently available micropower devices, we can further understand how to make improvements to the present technology. In particular, the present efficiency of micropower generators that are being developed is still relatively low. Therefore improving the efficiency will greatly enhance the development of micropower devices.

1.2. Significance and need for micropower device

During the mid to late 1990s, Epstein and Senturia [2] first suggested the concept of a micro-heat engine and Power MEMS to describe micro-systems, which can generate power or pumped heat. Since then, all kinds of micro-devices have been developed rapidly around the world. The interest in producing miniaturised mechanical devices has opened up new opportunities for micropower generation, because of the need for power supply devices with high specific energy (small size, low weight and long duration). Micro-gas turbine engines [3], micro-rotary engines [4], micro-thermoelectric systems [5] and micro-fuel cells [6] are typical micropower systems being developed. However, the miniaturisation of these devices is very much limited by the currently available power supply system. Despite the rapid miniaturisation of numerous electromechanical and mechanical engineering devices, the size, weight and energy storage capabilities of electrochemical batteries cannot be compromised. They occupy a significant fraction of both mass and volume of the entire device, thus greatly affecting both the design and specifications (Fig. 1).

There has been strong interest in both military and civilian applications for an alternative power generation system.

Fig. 1. Typical variations of electrochemical batteries [10].

A breakthrough in micropower generation technology will enable a rapid development of various micro-electronics, micro-mechanical, and electromechanical engineering devices for the next generation. Recent developments in wireless micro-systems, which are laying the groundwork for the next generation sensing systems, are also hindered by the absence of a tiny but powerful energy source [7]. There are many industries all over the world exploiting the technology of a micro-scale power system to enable developments in their specific fields. Availability of micropower devices also broadens the possibilities of using self-sustaining devices in remote or difficult-to-access locations. The ever-increasing use of portable electric and electronic devices also increases the need for efficient autonomous man-portable micropower supplies. Some of the most important potential applications include:

1. *Portable electronics*. Cellular phones, notebook computers, PDAs/palmtops, various hand-held devices, etc.
2. *Wireless equipments, sensors and communication systems*. Remote controls.
3. *Micro-air and space vehicles*. Miniature rockets for micro-satellites, micro-unmanned aerial vehicles, micro-rovers, etc.
4. *Military and security*. Portable cells for soldiers (signal sets, radios, etc.), micro-scouting vehicles, remote alarms, etc.
5. *Micro-climate control*.
6. *Other micro-devices*. Micro-pumps, micro-motors, micro-robots, micro-turbines, micro-thrusters, automobiles, etc.

1.3. Current situation (batteries)

Before attempting to develop new micro-scale power supplies, it is natural to investigate the currently available technologies. Currently, batteries are the predominant technology in most modern day applications. However, the use of batteries for micro-devices has presented various disadvantages. Batteries have a substantial environmental impact, high cost, and most importantly, a relatively low gravimetric ($Wh\,kg^{-1}$) and volumetric ($Wh\,L^{-1}$) energy densities. State-of-the-art primary batteries reach up to $1300\,Wh\,L^{-1}$ and $700\,Wh\,kg^{-1}$ and rechargeables up to $400\,Wh\,L^{-1}$ and $300\,Wh\,kg^{-1}$ [8]. The upper limit on battery performance has now been reached, as most of the materials that are practical for use as active materials in batteries have already been investigated and the list of unexplored materials is being depleted [9].

1.4. Potential solutions for micropower generation

The use of combustion processes for electric power generation (or micro-combustion) is known to have enormous advantages over conventional electrochemical batteries in terms of power generation per unit volume and energy storage per unit mass, even when the conversion efficiency in the combustion process from thermal energy to electrical energy is taken into account [11]. Considerable interest has arisen in the last few years in the miniaturisation of combustors (micro-combustors) as components of energy conversion systems, aiming at the possible replacement of conventional batteries with liquid fueled ones [12]. The primary incentive is the very high energy density of liquid fuels with respect to conventional batteries. Even accounting for a rather inefficient overall conversion of chemical energy to electricity, a liquid fuel approach in combustion would be superior by at least one order of magnitude, not to mention the advantage of the ease of recharging the "battery" [13]. Micro-combustion research has also led to the emergence of a new class of micro-electromechanical system, or simply Power MEMS, which utilises the high energy density of liquid hydrocarbon fuels. Both hydrocarbon fuel and Power MEMS will be described in the following sections (Sections 1.4.1 and 1.4.2).

1.4.1. Hydrocarbon fuel

The micro-combustion process will essentially make use of hydrocarbon as fuel. This is because even modern state-of-the-art batteries such as lithium-ion will not come close to producing potential energy densities that can be reached through the thermal conversion of hydrocarbon fuels. Hydrocarbon fuels provide energy storage of typically $45\,MJ\,kg^{-1}$, whereas the top batteries currently available (lithium-ion) provide only about $0.50\,MJ\,kg^{-1}$. Even at only 10% conversion efficiency from thermal to electrical energy (losses associated with extracting power from the fuel), hydrocarbon fuels still provide more than 10 times higher energy storage density than batteries [11], not to mention that they are easily replaceable.

Fig. 2 shows the potential advantage of using liquid hydrocarbon combustion to produce power by comparing the specific energy for *iso*-octane and several primary and secondary battery

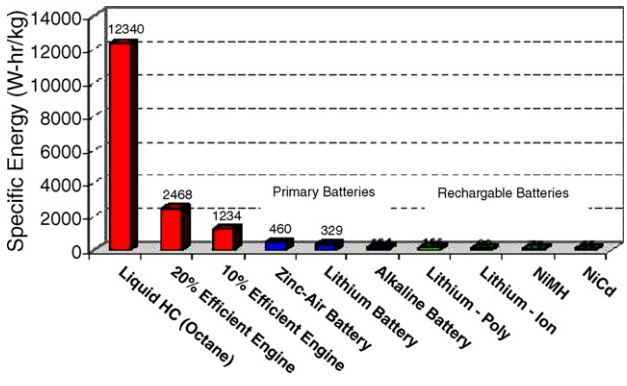

Fig. 2. Specific energy for liquid hydrocarbon (octane), 10% and 20% efficient engines, and several primary and secondary battery technologies [12].

technologies. The outstanding specific energy density of liquid hydrocarbon as compared to the conventional electrochemical batteries is clearly shown.

The advantages of hydrocarbon fuels also include low cost, constant voltage, no memory effect and instant rechargeability. Also, the shelf life of chemical fuels is in most cases very long, while batteries have a more limited shelf life. A micro-scale power device that could harness the chemical energy of hydrocarbon fuel would enable significant increases in the power output and the endurance of micropower devices. Therefore, taking advantage of the high energy density of a hydrocarbon fuel in a micro-combustion process becomes an attractive technological alternative in micro-scale power generation.

1.4.2. Power MEMS

The growing need to reduce system weight, increase operational lifetime as well as reducing unit cost has led to the introduction in the new field of high specific energy micro-electromechanical power systems, or simply, Power MEMS. The term "Power MEMS" was first suggested by Epstein and Senturia [2] in mid-1990s at the Massachusetts Institute of Technology, where they continued to study MEMS-based gas turbine generators [3]. Power MEMS describes the micro-systems which generate power or pumped heat. The concept behind this new field is to utilise the high energy density of liquid hydrocarbon fuels. Therefore, a miniaturised device even with a relatively inefficient conversion of hydrocarbon fuels to power would result in the increased lifetime of an electronic or mechanical system. Such micropower generators are characterised by thermal, electrical, and mechanical power density of approximately 1–20 W in sub-centimeter-sized packages [2]. Recently much attention has been focused on the application of MEMS devices to the production of electrical power. The ultimate goal would be to have "power generation in a chip". Many groups involved in Power MEMS are investigating scaled-down versions of well-established macro-scale combustion devices (internal combustion engines, gas turbines, pulsed combustors, etc.) [11]. The Power MEMS system has evolved into a much broader concept which includes other traditional thermal cycles, new heat engine concepts which may only be attractive at micro-scale, energy harvesting schemes, and even micro-fuel cells.

Due to the fact that electric power output levels of Power MEMS devices ranges over a broad spectrum, it has the potential to fulfill numerous applications. At the higher power range (of order 1–50 W), Power MEMS devices are envisioned to provide portable power for computers and other personal electronics, with both military and commercial applications. At the lower power range (of order 1 mW), Power MEMS devices could power remote sensors or actuators [14]. Emerging applications such as wireless sensing, wearable computing, autonomous robots, and other systems will require even more efficient power sources to deliver revolutionary new functionality and convenience. However, for the device to be practical, it must perform better than available batteries, with the performance metric typically being some form of energy density.

1.5. Summary of micropower technology

As mentioned earlier, the interest in producing miniaturised mechanical devices has open many new opportunities for micropower generation, because of the need for power supply devices with high specific energy (small size, low weight and long duration). More and more groups and researchers around the world are focusing on the study of micropower devices. As a result, many technologies of generating micropower have been developed recently. Some of the typical micropower systems include:

1. Micro-gas turbine engines [3] and micro-rotary engines [4].
2. Micro-thermoelectric systems [5].
3. Micro-fuel cells [6].
4. Micro-electromagnetic systems.
5. Micro-thermophotovoltaic systems [7].

All the above micropower systems will be described in greater detail in Section 2.

1.6. Outline of this review

The objective of this review is to cover the currently available or under development micropower devices. This will enable us to further understand and make improvements to present technology, in particular the efficiency of the devices.

Section 2 of this report has more in-depth details of the different technologies of micropower generation as listed in this section. Section 3 introduces the concept and principles of a thermophotovoltaic (TPV) system as a means of producing micropower. Section 4 focuses on the design, development and fabrication of the micro-TPV power generator. In Section 5, possible improvements in the efficiency of a micro-combustor as well as the overall efficiency of the micro-TPV power device are addressed. Recommendations for future works are made.

2. Approaches to micropower generation

2.1. Types and examples of micropower generation devices

Over the last decade, numerous micropower generation technologies have emerged due to the ever-increasing popularity of producing power on a micro-scale. The various technologies for micropower generation were listed earlier in Section 1.5. Firstly, there are the micro-gas turbine engines [3], micro-rotary engines [4], as well as the micro-free piston knock engines [15]. These micropower generators however feature a high-speed moving part. To eliminate moving parts in micropower sources, studies of direct energy conversion methods on the micro-scale are made. These include micro-thermoelectric [5], micro-fuel cells [6], micro-electromagnetic, and micro-thermophotovoltaic systems [7]. Each of these micropower generation technologies will be briefly described in the following sections. Examples of each micropower device being developed will also be discussed and reviewed.

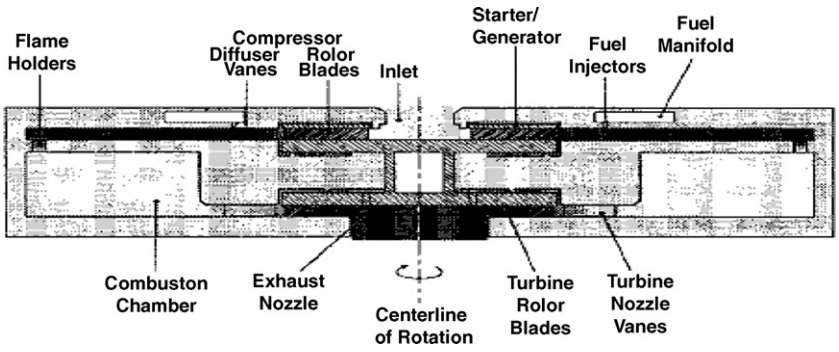

Fig. 3. The cross-section of the micro-gas turbine generator developed by MIT [3].

2.1.1. Micro-gas turbine engines and micro-rotary engines

The micro-gas turbine engine is one of the typical micropower devices being developed by Massachusetts Institute of Technology (MIT) [3], with the aim of producing 10–50 W of power from a turbine the size of 2.1 cm × 2.1 cm × 0.38 cm. The design uses six individual layers of silicon, with the turbine, combustor and housing all being made of silicon. The baseline engine design is illustrated in Fig. 3.

The engine mainly consists of a supersonic radial flow compressor and turbine connected by a hollow shaft. The system is targeted to operate at a tip speed of 500 m s^{-1}. However, the high rotor speed poses a great challenge to the fabrication and assembly of the system. So far, no prototype engine has been reported to produce a net power output.

The micro-rotary engine is another kind of micropower device proposed by the University of California at Berkeley [4]. The system is illustrated in Fig. 4. The engine, with a displacement of 0.064 mm^3, is targeted to produce a power output of 13.9 W, at a speed of 30,000 rpm with a 1 mm rotor. Using a rotary design without valves helps simplify the design of the micro-device, as sealing and actuation of micro-valves requires substantial complexity. The engine ultimately produced a 2.7 W of net power output due to some reasons such as fabrication and assembly.

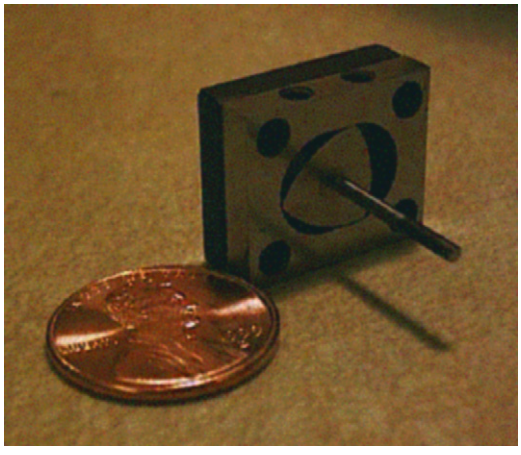

Fig. 4. The MEMS rotary engine developed by University of California at Berkeley [16].

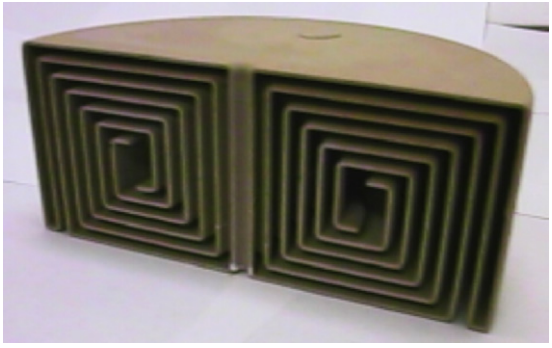

Fig. 5. The 'Swiss Roll' burner design of the micro-thermoelectric device developed by Sitzki et al. [5].

2.1.2. Micro-thermoelectric

The two kinds of micropower devices described in Section 2.1.1 have a high-speed shaft, which increases the difficulties of fabrication and assembly drastically. To eliminate the moving parts, Sitzki et al. [5] from University of Southern California developed a micro-thermoelectric device. The focus of the system is a 'Swiss roll' design of the burners as illustrated in Fig. 5. It works by allowing heat to be exchanged between the product and reactant streams. The counter-current heat exchanger design greatly reduces heat loss to the environment. The total reactant enthalpy is higher for the preheated reactants than for a cold incoming stream and thus preheated reactants can sustain combustion under conditions in which a flame without recirculation would be extinguished. By coupling this burner with a thermoelectric generator, electric power could be produced. The system is targeted to generate an electric power output of 0.1 W in a volume of 0.04 cm^3. The power density generated by the micro-thermoelectric system is significantly lower compared to the first two kinds of micro-engines. However the reliability is much higher since there is no moving part.

2.1.3. Micro-fuel cell

Fuel cells are steady-flow devices that accept fuel and oxidizer and therewith produce the reaction products as well as direct current (dc) electric power [17]. Currently, fuel cells that are being developed for portable applications are categorised in two types: DMFC (direct methanol fuel cells) and micro-PEFC (polymer electrolyte fuel cells). Both types follow the

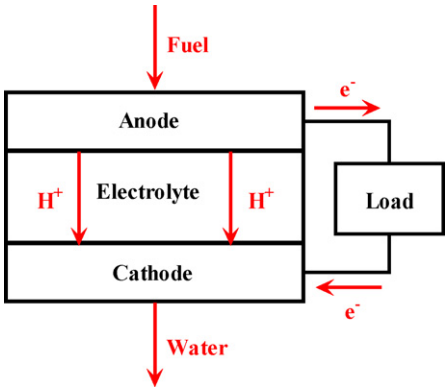

Fig. 6. The schematic view of a fuel cell [18].

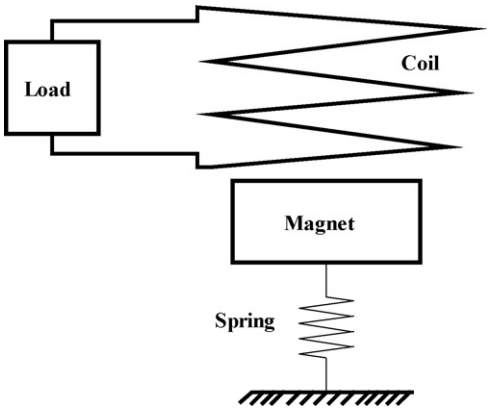

Fig. 7. The schematic view of an electromagnetic system [18].

same principle, as illustrated in Fig. 6. Fuel is supplied to the anode of the fuel cell and decomposed into protons and electrons under influence of a catalyst. The protons travel through an electrolyte, which passes the protons and stop the electrons from going through to the cathode. At the cathode, the protons and electrons combine with oxygen and generate water. The anode is connected through a load with the cathode, electrons travel to the cathode and reform with protons and oxygen to water, thus extracting electric power from the cell. A micro-fuel cell array is being developed by Lee et al. [6] from Stanford University. The system has integrated series connection of polymer electrolyte fuel cell in a planer array. The characteristic feature is the flip-flop configuration of the series path, where the interconnections of electrodes are from two different cells on the same side of the membrane. The design is particularly favorable for miniature fuel cells and has been prototyped using a variety of etch and deposition techniques adopted from microfabrication. It was reported that the peak power of the system exceeded 40 mW cm^{-2}.

2.1.4. Micro-electromagnetic

Most of the electromagnetic Power MEMS are based on a magnet mounted on a spring. The magnet follows a path through a coil when excited by ambient vibration. This movement will induce a voltage over the coil and when a load is connected, electric power can be extracted [18]. A schematic overview, represented in theory by a mass-spring-damper system, is illustrated in Fig. 7. Some examples that are fabricated are a microphone (which can generate up to 20 μW) or a device that works by a human walking motion (up to 400 μW) [19].

2.1.5. Micro-thermophotovoltaic (micro-TPV)

The thermophotovoltaic system (TPV) consists of four elements: the heat source, a micro-flame tube combustor (emitter), the filter and the low band gap photovoltaic array [7]. A fuel is combusted in a micro-combustor. When the emitter is heated to a sufficiently high temperature, it emits photons. When the photons with greater energy than the band gap of the PV cells, impinge, they cause free electrons to be produced and an electrical power output. The process is illustrated in Fig. 8. The National University of Singapore has constructed a micro-TPV system [7] that consists of a SiC emitter, a nine-layer dielectric filter and a GaSb PV cell array. They are capable of producing 0.92 W of electrical power with open-circuit voltage 2.32 V and short-circuit current 0.52 A. The combustor has a volume of 0.113 cm^3 and uses hydrogen at a rate of 4.2 g h^{-1} with H_2/air ratio of 0.9. This micro-TPV power device will be the main focus of study in this report. Section 3 will look into the in-depth details of such system.

2.2. Problems with micro-scale combustion and power generation

Most of the micropower technologies and devices reviewed in the earlier part of this section made use of micro-scale combustion to generate power. Although the introduction of micro-scale combustion to produce energy for micropower generation devices is becoming increasingly popular, it does present various problems and significant technological challenges. From a combustion viewpoint, the main challenge is primarily to burn cleanly and efficiently minute liquid flow rates in a confined space. However, when the approach is pursued at the micro-scale, issues of heat loss and quenching would also come to the fore. Other problem such as the fabrication, assembly and sealing of the micropower device (or micro-combustor) also poses a great challenge. These issues will be discussed in the following sections.

2.2.1. Heat loss and quenching

Combustion in micro-scale systems present problems related to the time available for the combustion reaction to occur and also to the possible heat loss and quenching of the combustion reaction by the wall [12]. The characteristic of the combus-

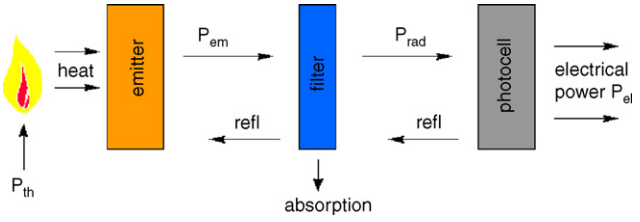

Fig. 8. The schematic layout of the thermophotovoltaic (TPV) power system [20].

tion reaction depends on the near-wall chemical kinetics, i.e. potential low wall temperature and radical depletion. The basic requirement for micro-combustion to occur is that the physical time available for combustion (residence time) must be larger than the time required for the chemical reaction to occur (combustion time). The realisation of high power density produced by the combustion reaction, however, requires effective completion of the combustion process within an extremely confined and small volume and is therefore fundamentally limited by the chemical reaction time constraints of the fuel. Tailoring the fluid flow to stabilise the flame and allow effective mixing of the cold reactants with the hot products is therefore critical to getting the fuel to completely react within a short time and constitutes a fundamental design challenge [3].

The chemical kinetic constraints are also exacerbated by the enhanced heat transfer effects that result from the large surface area-to-volume ratio of micropower devices. While many miniature space and air-breathing propulsion system concepts as well as micropower generators such as micro-gas turbine engines [3] and micro-rotary engines [4] have been proposed, most require moving parts. All miniaturised propulsion devices with moving parts experience more difficulties with heat and frictional losses due to the higher surface-to-volume ratios than their macro-scale counterparts. The surface-to-volume ratio is proportional to the inverse of the hydraulic diameter of combustor. According to the cubic-square law, when the size of a combustor decreases by a factor of 100, the surface-to-volume ratio will increase by a factor of 100 [21]. At the micro-scale, due to the high surface-to-volume ratio, heat loss through the wall of the combustor increase drastically, which tends to suppress ignition and quench the reaction. Not only does this high heat loss make it impossible to achieve conventional combustor efficiencies in excess of 99.9%, but it also increases chemical reaction times by lowering the temperature of the flame stabilization zones. The coupling between the fluid dynamics, heat transfer, and chemical kinetics is therefore much more pronounced for these small systems and is a critical element of the design process [3]. At the system level, these aforementioned chemical and thermal management problems could be exacerbated to the point that the whole concept may become unfeasible.

2.2.2. Fabrication and materials

The design of the micro-combustion power generation device is further complicated by the additional factor of fabrication and materials constraints. Sealing, fabrication and assembly of micro-combustor are much more difficult at small scales, because micro-fabrication processes have much poorer relative precision than convectional macro-scale processes [22]. The difficult operating environment of the micro-combustor also poses higher requirements to the selection of materials. Proper and careful selection of materials with high temperature tolerances and also good heat emission is required. Also worth mentioning is the ability of materials (such as silicon micro-fabrication) to overcome the complicated 3D geometries of the micro-combustor. The design of a micro-combustor therefore mandates careful and precise micro-fabrication, which is instrumental to achieving the economy and high tolerances necessary to make a micro-combustor viable.

2.3. Summary of micropower approaches

All the above-discussed micropower generation techniques are interesting and under extensive development in the world. We selected the micro-thermophotovoltaic (TPV) system for further in-depth review, due to our biased interest in direct energy conversion as well as recent rapid development in this area.

3. Introduction to thermophotovoltaic system

3.1. Background

The original thermophotovoltaic (TPV) concept was first proposed during the early 1960s. One of earliest discussions of the concept of TPV is done by White et al. [23] in their review of a wide range of advances in thermal energy conversion. However, it is only in recent years that technological improvements in the field of selective emitter and low band gap PV cells have evoked a renewed interest in TPV generation of electricity [24]. This section will introduce the methodology and concept of the TPV system, explaining how the system is functioned. The subsequent design of the micropower device that will be reviewed for this report will be based on this principle.

3.2. Principle of thermophotovoltaic (TPV) system

The basic principle of thermophotovoltaics (TPV) is the direct conversion of thermal energy into electricity without involving any moving parts. The TPV system basically consists of four essential components. They are the heat source, a selective emitter, a filter system and a low band gap photovoltaic converter [7]. The conceptual schematic layout of a TPV system is illustrated in Fig. 9.

As illustrated in Fig. 9, some various possible heat sources for the system include concentrated solar energy, the combustion of various fuels, and nuclear decay. When the heat source generates heat energy from either combustion, solar or nuclear, this heat energy will be absorbed by the selective emitter. When the emitter is heated to a sufficiently high temperature, it will emit photons. Thus, the selective emitter is used to convert heat from the source into radiation. The emitter can be made from broadband materials such as silicon carbide (SiC), or selective emitting materials such as $Er_3Al_5O_{12}$ (erbia), Co/Ni (cobalt/nickel)-doped MgO (magnesium oxide), Yb_2O_3 (ytterbia) or surface micro-structures by means of micro-machining [25,26]. The spectrums of broadband emitters usually operate at temperatures around 1000–1600 K. When the photons emitted from the emitter are impinge on the PV array, they evoke free electrons and produce electrical power output. Thus, the photovoltaic converter functions to convert heat radiation into electricity.

However, only those photons radiated by the emitter having energy greater than the band gap (e.g. for GaSb cells, it is 0.72 eV, corresponding to a wavelength of 1.7 μm) of the photovoltaic cell can be converted into electricity. In another words,

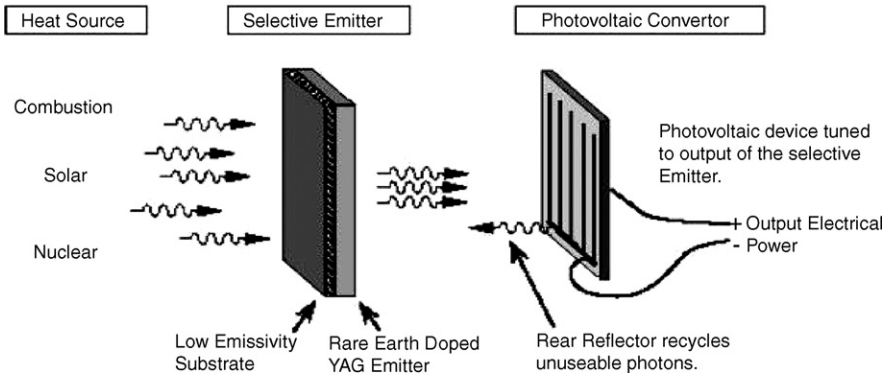

Fig. 9. The conceptual schematic layout of the thermophotovoltaic (TPV) power system [7].

those photons with a wavelength longer than 1.7 μm cannot generate free electrons and produce electricity when impinging on the photovoltaic cell [28]. If these photons are not stopped, they will be absorbed by the PV cells and subsequently result in a destructive heat load on the system components, which will lower the conversion efficiency of the system. As such, these photons should be sent back to the emitter in order to improve the system. Thereby, a filter is often employed in the design of conventional TPV systems. It serves to recycle and reflect back all the sub-band gap photons with too low energy and transmits all convertible to the PV array. However, in the micro-TPV system, the existence of a filter will complicate the fabrication and enlarge the volume of the system.

3.3. Efficiency of thermophotovoltaic (TPV) system

The overall efficiency of a conventional thermophotovoltaic (TPV) system is the product of the efficiencies of the PV cells, an optional filter, and the radiation source, consisting of the burner and the emitter, as follows:

$$\eta_{TPV} = \eta_{RS} \times \eta_{F} \times \eta_{PV}$$

where the subsystem efficiencies are defined as follows: η_{RS} is the net radiation power emitted by emitter/chemical energy input flow, η_{F} the radiation power absorbed in PV cell/net radiation power emitted by emitter and η_{PV} is the electrical output power/radiation power absorbed in PV cell. The net radiated power is defined as the total emission (whole spectrum) minus the radiation returned (e.g. from a reflecting optical filter) and absorbed in the emitter. The PV efficiency depends not only on the quality of the cell itself, but also on the shape and power density of the spectrum absorbed in it [29].

3.4. Advantages of thermophotovoltaic (TPV) system

The thermophotovoltaic (TPV) system promises to be a very clean and quiet source of electrical power with no moving parts and high power density, using a wide variety of energy source. Unlike the scaled-down versions of many macroscale heat engines, these advantages would be well inherited or even become outstanding at micro-scale level [30]. The system is simple (it does not involve many parts and components) yet effective. In terms of fabrication and assembly, it is also relatively easy. As a result, it can be more commonly used in commercial electronics and micro-devices, for which convenience and inexpensive production, reliable operating, and low maintenance cost are the key to success. It has a very good potential as a replacement for traditional batteries. Other advantages are those commonly applicable to micropower devices as described in Section 1.4 earlier.

4. A micro-thermophotovoltaic power device

4.1. Introduction

This section aims to review in detail a micropower device based on the principle of thermophotovoltaic (TPV) system. The concept and theory behind the TPV method of power generation discussed in Section 3 has been implemented into the design, development and fabrication of the micro-TPV power generator. Each individual component of the device will be looked into. This includes the heat source (micro-combustor), SiC emitter, dielectric filter, GaSb photovoltaic (PV) cell array and the cooling fins. Other major issues concerning the design of the micro-TPV power generator such as combustion in the micro-cylindrical combustor, effect of wall thickness of micro-combustors (on the performance of the system), and the effect of step height (of the micro-combustor) on wall temperature, will also be reviewed. It must be acknowledge that a large part of the contents of this section is developed based on the detailed reviewing of a novel concept of a micro-thermophotovoltaic (micro-TPV) power generator [7] currently under research and development by the collaboration of the National University of Singapore and the California State Polytechnic University (Fig. 10).

4.2. Design and structure of the micro-TPV power device

The design of the micro-TPV power device comprises mainly of four main components: (1) a heat source; (2) a micro-flame tube combustor (the wall of the micro-combustor will be a broadband emitter); (3) a simple dielectric filter; (4) a PV cell array. Furthermore, micro-cooling fin arrays are also attached on the back of the PV cells to remove the sink heat by the PV cells.

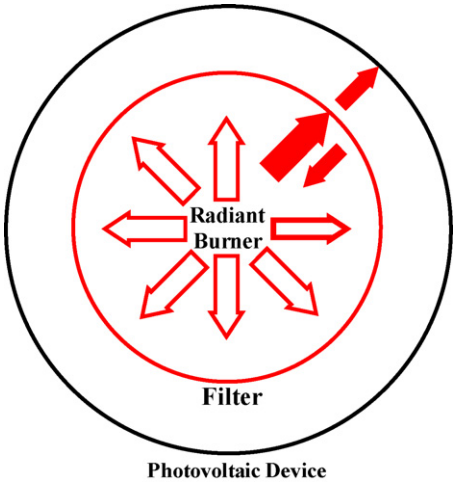

Fig. 10. The conceptual schematic cross-section of a typical thermophotovoltaic (TPV) power system [27].

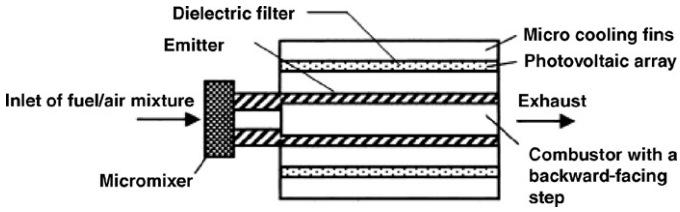

Fig. 11. The schematic layout of the micro-thermophotovoltaic (micro-TPV) power device [30].

All these components are integrated together to form the general structure of the micropower device. The schematic layout of the micro-TPV power device is illustrated in Fig. 11. Each of these components will be described in more details in Section 4.4. A prototype of this micro-TPV power generator has been build up and tested in the National University of Singapore (NUS) [21]. To give a better picture of the structure of the micro-TPV power device, a schematic cross-sectional view of the device (view from the front) is also illustrated in Fig. 12. The cooling fins are not included in the illustration.

4.3. Operating principles of the micro-TPV power device

The micro-thermophotovoltaic (micro-TPV) system is a micropower generator which uses photovoltaic (PV) cells to convert heat radiation (from the combustion of hydrocarbon fuel) into electricity. The general operating principle of the device is as follows: hydrocarbon fuel first mixes with compressed air in the micro-mixer. The mixture then enters a cylindrical micro-combustor, where the combustion takes place. As the wall of the micro-combustor is heated to a sufficiently high temperature, it emits a lot of photos (as radiation) from a broadband emitter. The broadband emitter is on the wall of the micro-combustor. The micro-combustor is peripherally enclosed by arrays of photovoltaic (PV) cells (as can be seen in Fig. 12), so that the radiative heat from the wall of the micro-combustor can be absorbed by the PV cells. The radiated photons interact with the electrons in the PV cells by imparting their energy to the electron as kinetic energy, which consequently produces an electric current. Hydrogen will be used as the hydrocarbon fuel for combustion (this will be addressed later in Section 4.4.1).

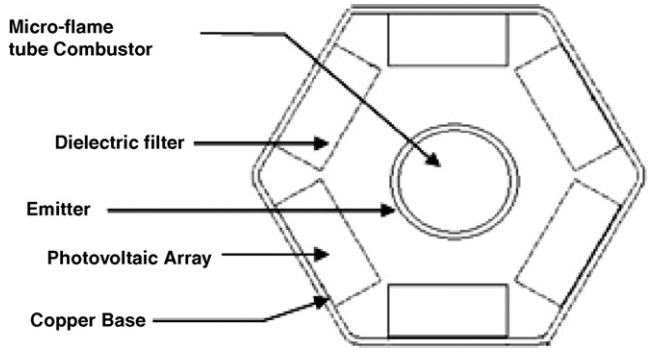

Fig. 12. The cross-sectional schematic layout of the micro-TPV power device.

4.4. Components of the micro-TPV power device

As mentioned in Section 4.2, the design of the micro-TPV power device comprises mainly of four main components: (1) a heat source; (2) a micro-flame tube combustor (the wall of the micro-combustor will be a broadband emitter); (3) a simple dielectric filter; (4) a PV cell array. This section will look into the design details of each of these components.

4.4.1. Micro-combustor

As one of the most important components of the micro-TPV power system, the micro-combustor must be developed first. Compared to conventional combustors, a micro-combustor is more highly constrained by inadequate residence time for complete combustion and high rates of heat transfer from the combustor. Some of the major challenges and problems with micro-scale combustion have been mentioned earlier in Section 2.2. For micro-TPV applications, the desired output is a high and uniform temperature along the wall of the micro-combustor.

The major challenge in the micro-combustor design is to keep an optimum balance between sustaining combustion and maximising the heat output [7]. A high surface-to-volume ratio is very favorable to the output power density per unit volume. However, a high heat output will affect the stable combustion in the micro-combustor (see Section 2.2.1). To verify the feasibility of micro-combustion and to optimise the design of the micro-combustor, a series of numerical simulations and experimental studies were carried out by Chou et al. from the National University of Singapore (NUS). These experiments include the testing of the feasibility of combustion in micro-devices and determine the relevant factors affecting micro-combustion (H_2/air ratio, flow rate of fuel, etc.) [31]. Details of the experiment will be explained later in Section 4.5.1. Other tests and investigation that were carried out include:

1. Effects of wall thickness of micro-combustor on the performance of the micro-TPV power device (see Section 4.5.2) [32],

Table 1
Key parameters and their values for the micro-combustor design

Micro-combustor parameters	Values
H_2/air ratio	0.9
Fuel flow rate	4.20 g h^{-1}
Backward facing step	10.0 mm
Step height	1.0 mm
Wall thickness	0.4 mm
Inner diameter	3.0 mm
Length	16.0 mm

2. Combustion in the micro-cylindrical combustor with and without a backward facing step (see Section 4.5.3) [28],
3. Effects of step height on wall temperature of the micro-combustor (Section 4.5.4) [33].

Based on all the above tests and investigation that was carried out, a micro-combustor is being designed for application to the design of the micro-TPV power device. The parameters for the micro-combustors were concluded in Table 1.

Fig. 13 shows the cross-sectional schematic layout of the micro-combustor design with the derived specifications. Investigation results indicate that a micro-cylindrical flame tube with the general shape of a backward facing step is one of the simplest, but all the same effective, structures for the micro-TPV application. The backward facing step can facilitate recirculation along the wall and enhance the mixing process around the rim of the tube flow. Thereby, a high and uniform temperature can be obtained along the wall of the micro-combustor.

Suitable dimensions for the design of the micro-combustor are a 10 mm backward facing step with a step height of 1 mm. The micro-combustor is designed to a length of 16 mm with an inner diameter of 3 mm and a wall thickness of 0.4 mm. These dimensions will result in a micro-combustor volume of 0.113 cm^3. Also, the micro-combustor is able to achieve an average temperature of 1325 K along the wall, and the biggest temperature difference is less than 5% when the H_2 flow rate is 4.20 g h^{-1} and the H_2/air ratio is 0.9. The efficiency of the micro-combustor is 19.5% [34]. The micro-combustor can be fabricated by casting, followed by polishing process to the outer surface.

In the micro-combustor design, the choice of fuel plays a key role. H_2 (hydrogen) is chosen as the fuel because of its original high heating value, rapid rate of vaporisation, fast diffusion velocity, short reaction time and high flame speed [4]. As the fuel mixture (H_2 and air) enters the micro-combustor, the combustion takes place near the wall rather than at the centreline of the flame tube at the beginning stage. The part of the H_2/air mixture around the central region is then heated and accelerated by combustion products surrounding it and flows quickly to near the end of the flame tube and combusts there, which inversely heats the gas near the wall, and therefore maintains a fairly uniform temperature along the wall [7]. More investigation on the combustion will be discussed later in Section 4.5.1 from a series of numerical simulations and experimental studies carried out by Chou and co-workers [31] from National University of Singapore.

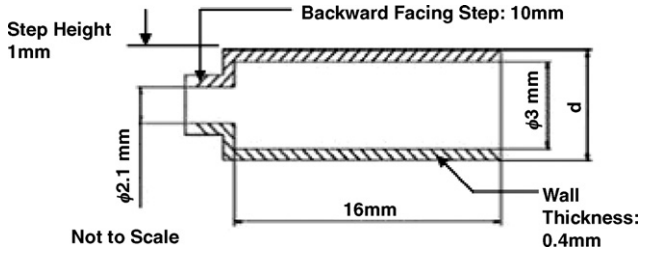

Fig. 13. The cross-sectional schematic layout of the micro-combustor.

4.4.2. SiC emitter

The emitter is another key component in the design of the micro-TPV power device. The emitter is the wall of the micro-combustor and it functions to convert heat energy from the combustion into radiation by emitting photons. There are basically two different types of emitters, namely broadband emitters and selective emitters. Blackbody is a typical broadband radiation materials, its emission behavior can be approximated by graphite or a soot-covered surface [34]. However, a broadband radiating material of practical importance is silicon carbide (SiC) with an emissivity $\varepsilon_{SiC} \approx 0.9$. While a selective emitter exhibits a high emittance in the spectral range usable for the PV cells, and a low emittance elsewhere. For the last decade, several methods have been developed to fabricate selective emitters. One familiar way is to use oxides of rare earth materials such as Er_2O_3 (erbia) and Yb_2O_3 (ytterbia) [35]. Another way is micro-structuring the surface of the emitters [36]. Recently, a new thermally excited Co/Ni (cobalt/nickel)-doped MgO (magnesium oxide) matched emitter [37] has been developed in University of Washington. This kind of emitters exhibits a better spectral efficiency.

The prototype micro-TPV power generator developed by Chou and co-workers [7] from the National University of Singapore uses silicon carbide (SiC) as the material for the emitter. SiC has been selected due to its good emissivity and high temperature reliability. Furthermore, compared with other selective emitters such as micro-machining tungsten and rare earth oxide, it is easier to fabricate into a cylindrical shape. The SiC emitter is a typical broadband emitter and the spectrum of broadband emitters generally operates at temperature of about 1000–1600 K.

As part of an effort to develop a suitable material for the emitter, Chou et al. from the National University of Singapore carried out a series of experiments to test the performance of a prototype micro-TPV power generator with different emitting materials [38]. The efficiency of the micro-combustor can be improved by replacing the SiC emitter with other selective emitters, which will consequently lead to a higher overall efficiency for the micro-TPV power generator. This will be discussed later in Section 5.

4.4.3. Dielectric filter

The next key component in the design of the micro-TPV power device is a simple nine-layer dielectric filter. As mentioned in Section 4.4.2, the SiC emitter is a typical broadband emitter. The spectra of broadband emitters operating at tem-

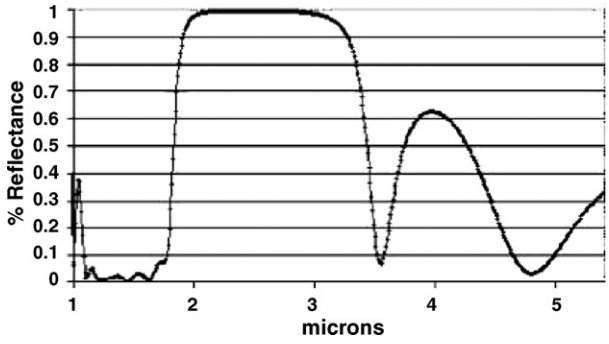

Fig. 14. The reflectance of the nine-layer dielectric filter [7].

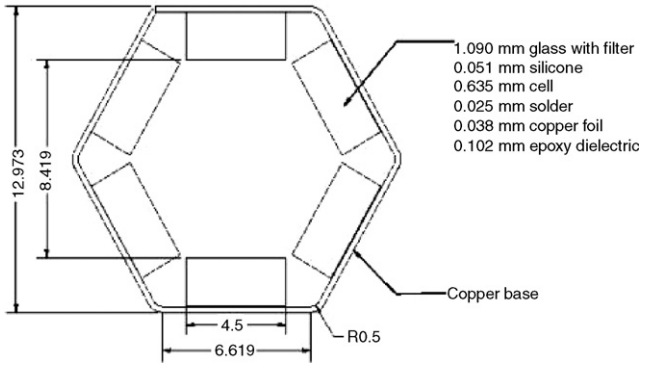

Fig. 15. The nine-layer dielectric filters bonded on the top of each hexagonal GaSb PV cells [34].

peratures in the range of 1000–1600 K contain a significant proportion of photons with energies not sufficient enough to generate charge carriers in the PV cells. As discussed earlier in Section 3.2, only those photons radiated by the emitter having energy greater than the band gap (e.g. for GaSb cells, it is 0.72 eV, corresponding to a wavelength of 1.7 μm) of the photovoltaic cell can be converted into electricity. In another words, those photons with a wavelength longer than 1.7 μm cannot generate free electrons and produce electricity when impinging on the photovoltaic cell [28]. These photos are called sub-band gap photons.

If this portion of energy is being absorbed by the PV cells, it will result in a destructive heat load on the generator components, subsequently lowering the conversion efficiency of the system. To improve the overall efficiency of the micro-TPV system, it is very important to recycle these photons. Therefore, a filter is required in the micro-TPV system (to filter out photons with wavelength longer than 1.7 μm).

The prototype micro-TPV power generator developed by Chou and co-workers [7] from the National University of Singapore employs a simple nine-layer dielectric filter for the micro-TPV system. The filter is able to recycle the energy emitted in the range of 1.8–3.5 μm mid-wavelength band, thereby improving the overall efficiency of the system [34]. The reflectance of the dielectric filter is shown in Fig. 14. The reflectance is measured with a customised in-house built optical test system done by the commercial fabricator (with an uncertainty of less than 3%). Ideally, the filter should be able to reflect all non-convertible photons back to the emitter and transmit all convertible photons to the PV cell array. However, this is very difficult to achieve in actual practice.

A commercial fabricator JX Crystals Inc. [39] was engaged by NUS for the fabrication of the nine-layer dielectric filter. The filter is fabricated with alternating layers of silicon and silicon dioxide. It is deposited on a glass slide with a conventional electron beam evaporation system and bonded on the top of GaSb PV cells with silicone, as illustrated in Fig. 15. This method makes the assembly of micro-TPV system very convenient.

4.4.4. Photovoltaic (PV) cell array

The next key component in the design of the micro-TPV power device is the photovoltaic (PV) cell array. Compared to the PV conversion of solar energy, the photons emitted from the heat source in the range of 1000–1600 K are distributed at much lower energies and longer wavelengths. This necessitates the use of low band gap semiconductors for the TPV energy conversion diode, in order to simultaneously maximise both the efficiency and the power density.

Although the concept of TPV energy conversion was first proposed in 1960s [23], it was only in recent years that technological improvements in the field of low band gap photovoltaic cells and high temperature materials have evoked a renewed interest in TPV generation of electricity [40]. Some typical low band gap PV cells developed recently for TPV applications are GaSb (gallium antimonide) [40], GaInAs (gallium indium antimonide) [41] and InGaAsSb (indium gallium arsenic antimonide) [42]. The prototype micro-TPV power generator developed by Chou and co-workers [7] from the National University of Singapore employs a GaSb PV cell array for the micro-TPV system, corresponding to the dielectric filter. The GaSb cell array is able to respond out to photons with wavelength less than 1.8 μm. Fig. 16 shows the quantum efficiency of the GaSb cell.

The technology used to form the pn-junction is based on a Zn vapor diffusion process into an n-doped GaSb substrate [43]. Thus, expensive epitaxial growth of thin semiconductor layers is successfully avoided. The Zn vapor diffusion process is performed in a so-called “pseudoclosed” box. The diffusion source is a mixture of Zn and antimony [34].

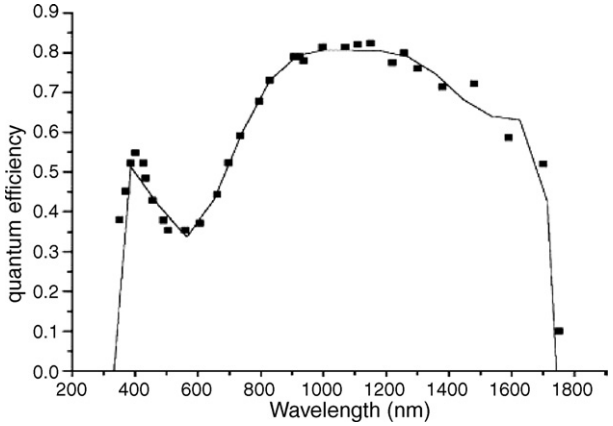

Fig. 16. The quantum efficiency of GaSb PV cells [7].

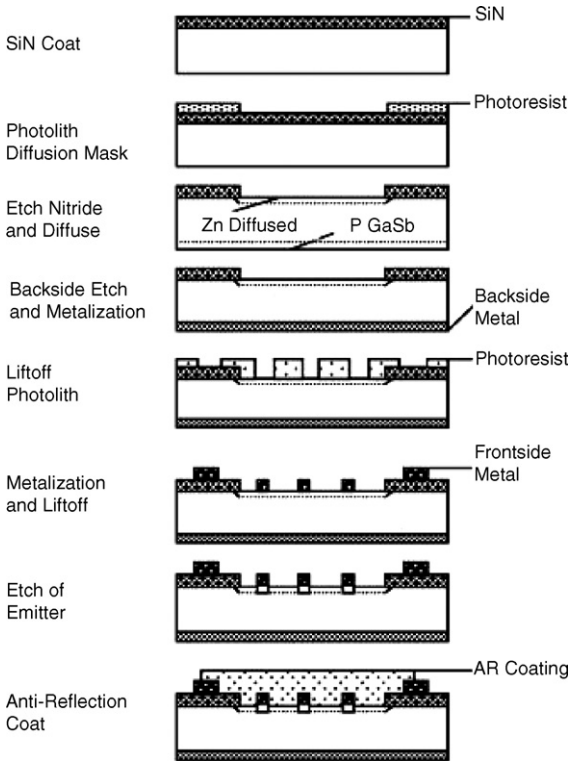

Fig. 17. The outline of the GaSb PV cell fabrication process [34].

4.4.4.1. Fabrication of the GaSb PV cell array. An n-type GaSb wafer doped with Te is first coated with a silicon-nitride diffusion barrier and standard photolithography is used to open holes in the dielectric. A pn-junction is then formed by zinc diffusion through the mask opening. The diffusion creates a Zn-doped p-type GaSb cell. The front patterned side of the wafer is then protected with photoresist; while the junction is removed from the backside of the wafer with a nonselective etches. The backside of the wafer is then metallised. The front-side metallisation area is defined by standard lift-off photolithography and metal evaporation. Finally, etching of the emitter and deposition of an antireflection (AR) coating are performed to maximize photocurrent [34]. The outline of the GaSb PV cell fabrication process is illustrated in Fig. 17.

4.4.4.2. Specifications of the GaSb PV cell array. Because of the nature that only planer-shape GaSb PV cells can be fabricated, multiple cell arrays will have to be formed together to generate the desired cylindrical shape. Therefore, the cylindrical PV cell array comprises of six 4.5 mm × 18 mm planer GaSb PV cells, forming the geometry of a cylindrical tube. The cylindrical PV cell array is illustrated in Fig. 18.

Fig. 19 shows the circuit board of the GaSb PV cell array, which is composed of the six 4.5 mm × 18 mm planar GaSb cells. The circuit board will be blended to form the hexagonal geometry as shown in Figs. 15 and 18. The active area is for each of the planer PV cell is 4.3 mm × 15.5 mm. The dielectric filters will be bonded on the top of the GaSb PV cells and the filter face-to-face distance is 8.419 mm. A commercial fabricator JX Crystals Inc. [39] was engaged by NUS for the fabrication of the GaSb PV cells (the same fabricator as the dielectric filter).

4.4.4.3. Performance of the GaSb PV cell array. The performance of the planar GaSb PV circuit is measured with a flash lamp solar simulator. The results indicate that the planar GaSb PV circuit offers a very good electrical conversion performance. The fill factor reaches 0.776. The plot of current versus voltage (*I–V* curve) of the circuit is shown in Fig. 20. The 'light' is a relative number used to normalise intensity during flash testing, by adjusting the 'light' intensity to obtain a certain current density [7].

4.4.5. Cooling fins

The operation temperature of the PV cells affects the overall power output of the GaSb TPV cell on band gap and reverse the saturation current. As the operating temperature increases, the conversion efficiency of the TPV cell will decrease. Therefore, effective cooling would be necessary in a GaSb TPV system. Arrays of cooling fins are attached on the back of the PV cells to remove the sink heat from the PV cells. The cooling fins can be made of highly conductive materials such as aluminium or copper. The fin surfaces can be manufactured by extruding or welding. The array of cooling fins will enhance the rate of heat transfer from the surface of the GaSb PV cells by several folds, by exposing a larger surface area to convection and radiation. Fig. 21 shows the array of cooling fins attached to

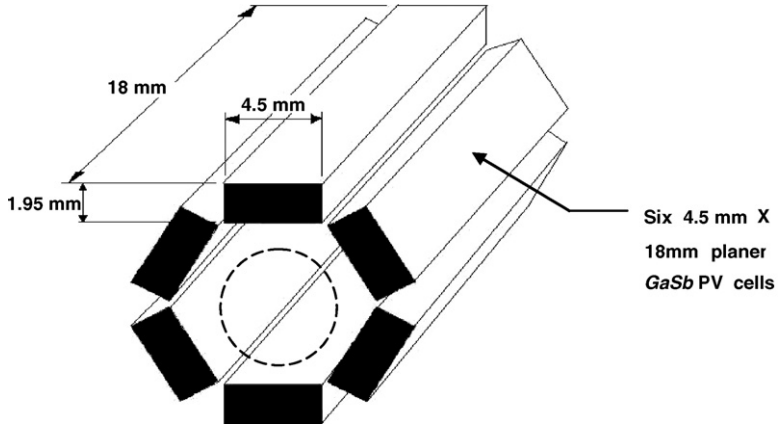

Fig. 18. The cylindrical PV cell array comprising of six GaSb PV cells.

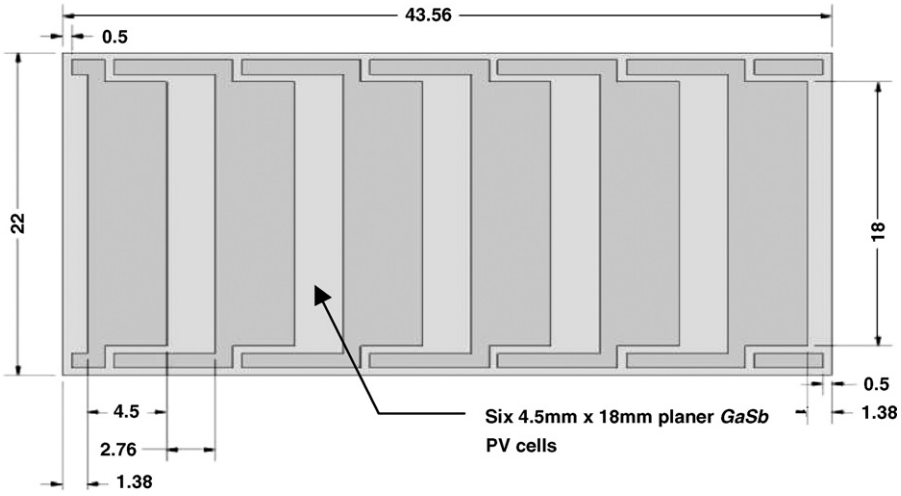

Fig. 19. The circuit board of the GaSb PV cell array comprising of six GaSb PV cells [34].

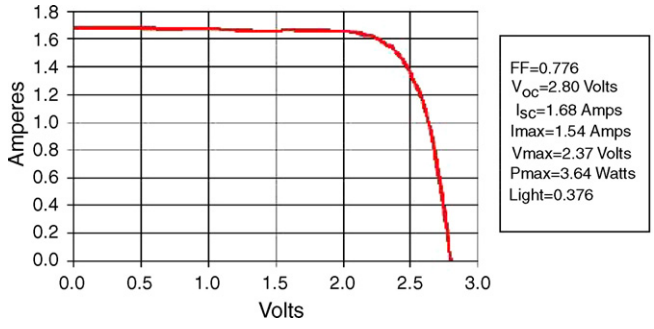

Fig. 20. The current vs. voltage (*I–V*) curve of the GaSb PV circuit [7].

a prototype micro-TPV power generator (without the micro-combustor) developed by Chou and co-workers [7] from the National University of Singapore.

4.5. Investigation and experimental studies

The micro-combustor and combustion process are components which affect the performance and design of the micro-TPV power device the most. This is due to the fact that almost all the problems and challenges facing the design of the device are associated with the micro-scale combustion for application to the TPV systems. Some of the general problems with micro-scale combustion and power generation are discussed earlier in Section 2.2. This section of the report will look at several investigations, numerical simulations, as well as experimental studies of various aspects of the design of the micro-TPV device concerning the micro-combustor and SiC emitter. It must be acknowledge that these investigations and experimental studies were conducted by Chou et al. [28,31–33,38] from the National University of Singapore. Results from these experimental studies will very much influence the design of the micro-combustor and emitter component of the micro-TPV power device.

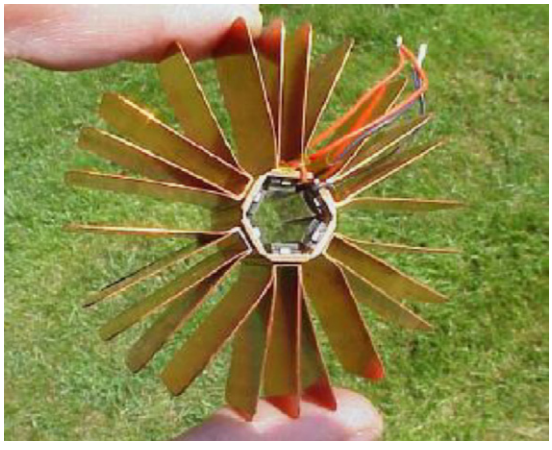

Fig. 21. Array of cooling fins attached on the back of the PV cells of the device [21].

4.5.1. Micro-combustion studies (flow rate and H_2/air ratio)

The first step on the micro-TPV power system was focused on the micro-combustors to ascertain that a stable flame could be obtained and radiative temperature along the walls of the micro-combustor is high enough to activate GaSb photovoltaic cells. Chou et al. from the National University of Singapore did an experimental study to observe the characteristic of combustion and how the H_2/air ratio and flow rate of fuel would affect the performance of combustion, and consequently the overall efficiency of the device.

A micro-combustion experimental rig was set-up for the test. It includes: (1) a micro-combustor, (2) a connection tube with four 0.2 mm-diameter orifices distributed equally around the perimeter, through which, high pressure hydrogen is injected into an air stream and mixed with air evenly, (3) a plenum filled with high pressure and uniform hydrogen and (4) two sets of electronic mass flow controllers, one is for hydrogen with a capacity of 1000 SCCM, and the other is for air with a capacity of 5000 SCCM. The two controllers are capable of controlling flow rates accurate to 1% of the full scale [28]. The combustion experiment set-up is illustrated in Fig. 22.

The proposed micro-combustor for the micro-TPV power device is mounted onto the experimental rig. The structures and

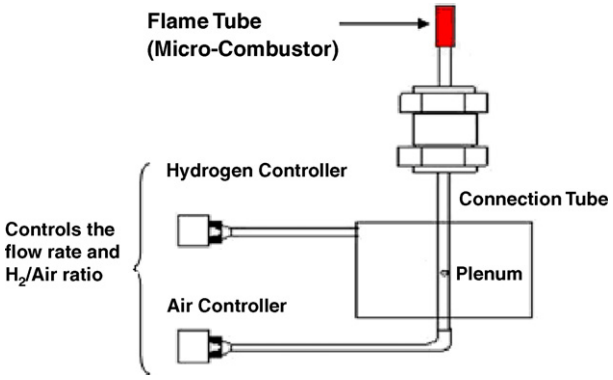

Fig. 22. The micro-combustion experimental rig to test the combustion characteristics [28].

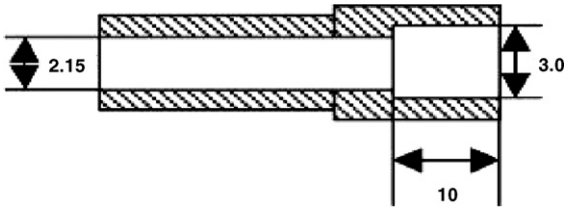

Fig. 23. The structures and dimensions of the tested micro-combustor [31].

dimensions of the proposed micro-combustor to be tested are illustrated in Fig. 23.

The hydrogen and air are premixed by the plenum before sending them to the proposed micro-combustor. The mass flow rates of hydrogen and air were controlled accurately by two sets of electronic mass flow controllers, through which H_2/air ratio can also be adjusted. The distributions of temperature both at the exit plane and along the wall of the proposed cylindrical micro-combustor were measured by 0.203 mm diameter type K thermocouples [30]. In this experiment, different flow rates and H_2/air ratio were tested in full range in which stable flame could be obtained inside the micro-combustor.

4.5.1.1. Effect of H_2/air ratio. Three different H_2/air ratios were being tested in the experiment. They are ratios of 0.45, 0.7 and 1.0. The flow rate of fuel at the inlet is maintained at 8 m s^{-1} for all three H_2/air ratios. The same proposed micro-combustor (see Fig. 23) is also used throughout all the three tests. Fig. 24 illustrates the combustion result of the micro-combustor, showing that an increase in the H_2/air ratios (from 0.45 to 1.0) results in a significant colour change on the wall of the micro-combustor, which quantitatively indicates the increase in temperature.

To further understand the characteristics of the combustion process as well as the temperature distribution within the micro-combustor, a numerical simulation was also carried out by Chou and co-workers [31], as shown in Fig. 25. The numerical simulation shows that the micro-combustor is able to obtained highest temperature (~1305 K) and also maintains an evenly distributed temperature along the wall of the combustor when the H_2/air ratio is at the highest value (at 1.0).

To conclude, the experiment shows that the completeness of combustion within the micro-combustor can be improve by increasing the H_2/air ratio. As shown in the plot in Fig. 26, the maximum electrical power output under different flow rate increase drastically when the H_2/air ratio increases from 0.5 to 0.9. This is due to the fact that more fuel is taking part in the combustion, subsequently increases the temperature along the wall of micro-combustor tremendously. However, when the H_2/air ratio increases further from 0.9 to 1.0, the maximum electrical power output increases very little (due to the minimal increase in wall temperature), as a result, it becomes negligible. Therefore, the micro-TPV system produces a better efficiency at H_2/air ratio of 0.9 than at 1.0. Thus, we can conclude that as the H_2/air ratio increases, the electrical power output increases.

4.5.1.2. Effect of fuel flow rate (V_{in}). Three different flow rates were also tested in the experiment. They are $V_{in} = 4$, 8 and 12 m s^{-1}. The H_2/air ratio is maintained at 0.6 for all three flow rates. The same proposed micro-combustor (see Fig. 23) is also used throughout all the three tests. Fig. 27 illustrates the combustion result of the micro-combustor.

Again, it shows that an increase in the fuel flow rate (from $V_{in} = 4$ to 12 m s^{-1}) will result in a significant colour change on the wall of the micro-combustor (see Fig. 27), which quantitatively indicates the increase in temperature. Based on Fig. 26 again, we can conclude that with the increase in fuel flow rate, the maximum electrical power output of the system increases with corresponding H_2/air ratio. This is because the increase in flow rate enhances the heat release rate, subsequently increasing

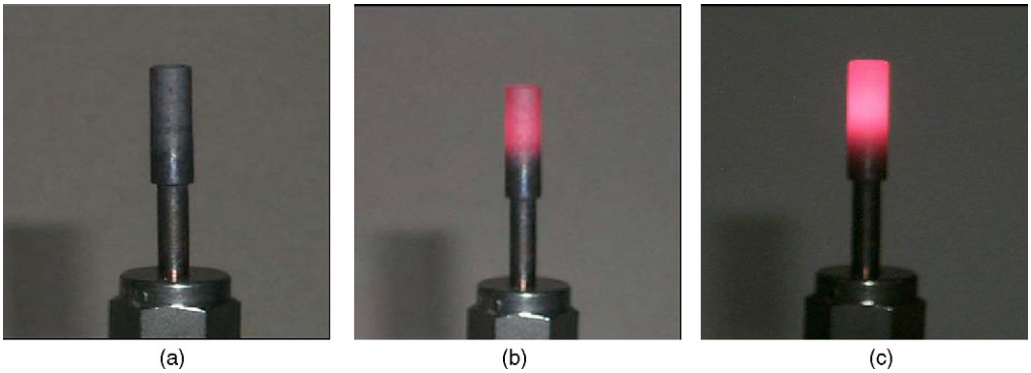

Fig. 24. Combustion observed on the micro-combustor at a flow rate of 8 m s^{-1} for different H_2/air ratio of (a) $\sigma = 0.45$, (b) $\sigma = 0.7$ and (c) $\sigma = 1.0$ [30].

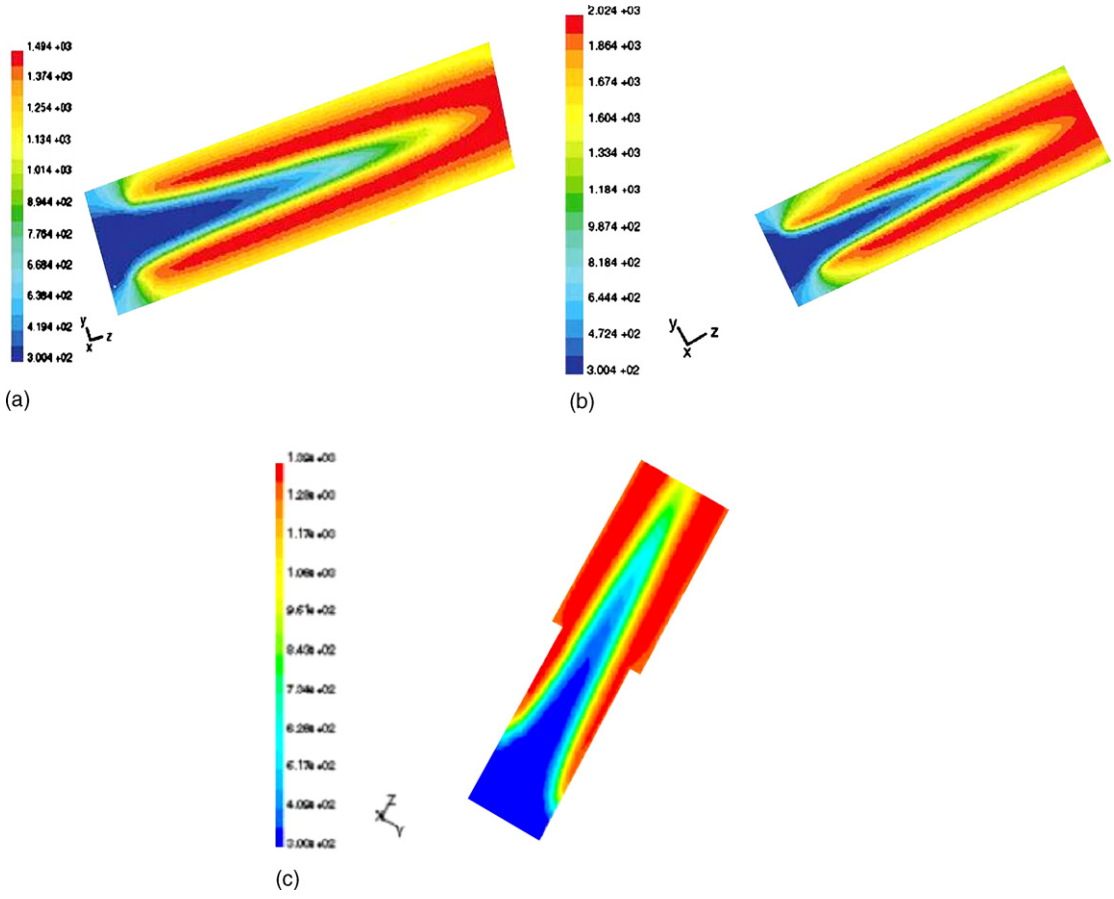

Fig. 25. The numerical simulation showing the temperature profile in the micro-combustor for different H_2/air ratio of (a) $\sigma = 0.45$, (b) $\sigma = 0.7$ and (c) $\sigma = 1.0$ [31].

the temperature along the wall of micro-combustor, leading to higher electric power output.

4.5.1.3. Conclusion from the combustion results. Based on the experimental studies on combustion behavior carried out by Chou and co-workers [31], we can conclude that external parameters such as H_2/air ratio not only affect the overall temperature, but also influence the temperature distribution and completeness of combustion. Flow rate is another important factor affecting micro-combustion in a flame tube. Increasing both the H_2/air ratio as well as flow rate will consequently lead to an increase in overall electric power output of the micro-TPV system (see Fig. 26). An average temperature of about 1305 K has been achieved along the wall of the micro-combustor based on a flow speed of 12 m s^{-1} at the inlet and a H_2/air ratio of 0.95. Therefore, these are the appropriate parameters that were used for the heat source as part of the design of the micro-TPV power device.

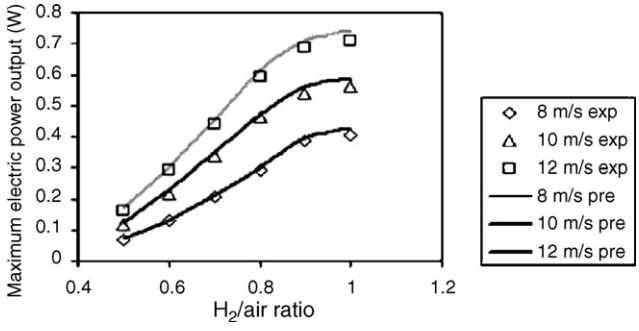

Fig. 26. The power outputs in a prototype TPV power system with different H_2/air ratio [30].

4.5.2. Effects of wall thickness of micro-combustor

Yang et al. [32] from the National University of Singapore carried out an experiment to observe the effect of wall thickness of micro-combustor on the performance of micro-TPV power generators. In the experiment, three kinds of micro-cylindrical SiC combustors with different wall thickness are being fabricated for testing. All three micro-combustors have a common inner diameter of 3 mm and a length of 16 mm. This corresponds to a common combustion chamber volume of 0.113 cm^3. The specifications of the micro-combustor are illustrated in Fig. 28. The outer diameter, d, is 3.8, 4.2 and 4.6 mm, respectively, corresponding to a wall thickness, t, of 0.4, 0.6 and 0.8 mm.

In the experiment, all the three micro-combustors with different wall thickness were incorporated into a prototype micro-TPV power generator. The electrical power output that is being produced with each of the micro-combustors is then measured for various flow rate and H_2/air ratio. Figs. 29 and 30 show the maximum electrical power output and the short-circuit current of the system under different wall thickness, respectively, when the flow rate at the inlet is kept as 12 m s^{-1}, and H_2/air ratio varies from 0.5 to 1.0.

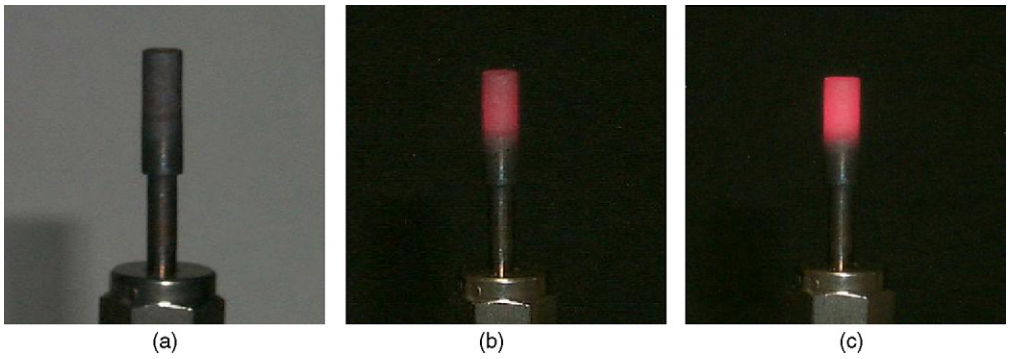

Fig. 27. Combustion observed on the micro-combustor at a H_2/air ratio of 0.6 for different fuel flow rates of (a) $V_{in} = 4\,m\,s^{-1}$, (b) $V_{in} = 8\,m\,s^{-1}$ and (c) $V_{in} = 12\,m\,s^{-1}$ [30].

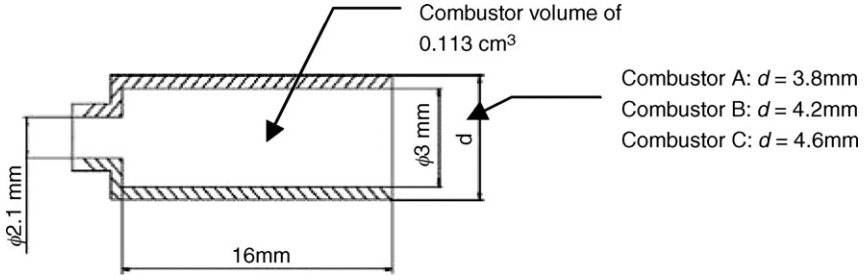

Fig. 28. The specifications of the micro-combustors that are being experimented [32].

The experimental results clearly indicate that with a decrease in the wall thickness of the micro-SiC combustor, both the maximum electrical power output and the short-circuit current increase drastically, especially at low H_2/air ratio (see Figs. 29 and 30). As the wall thickness decreases from 0.8 to 0.6 mm, the maximum electrical power output and short-circuit current increases by more than 36 and 34%, respectively. When the wall thickness is further decrease from 0.6 to 0.4 mm, the increase in maximum electrical power output and short-circuit current is also evident but relatively lower. The increase in the open-circuit voltage is insignificant in this case.

With respect to the H_2/air ratio, Figs. 29 and 30 show that both the maximum electrical power output and short-circuit current under different wall thickness increase drastically when the H_2/air ratio increases from 0.5 to 0.9. As for the flow rate, result indicates that the maximum electrical power output of the system under different wall thickness increases almost linearly with the increase in flow rate. Fig. 31 shows the performance curves of the micro-TPV system with different wall thickness, when the H_2/air ratio is kept as constant at 0.9, and flow rate varies from 8 to 12 m s^{-1}.

In terms of the effect of wall thickness on the wall temperature of the micro-combustor, it was realised that the mean wall temperature increases with the decrease in wall thickness, as can be seen in Fig. 32. This is even more evident when the wall thickness decreases from 0.8 to 0.6 mm. This variation is in correspondence with the variation rule of temperature along the wall of micro-combustor.

4.5.2.1. The effect of wall thickness. To conclude, the analysis shows that with the decrease in wall thickness, the maximum

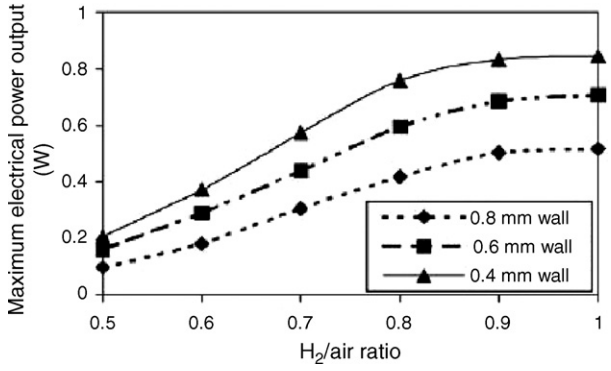

Fig. 29. Maximum electrical power output under different H_2/air ratio at flow rate of 12 m s^{-1} [32].

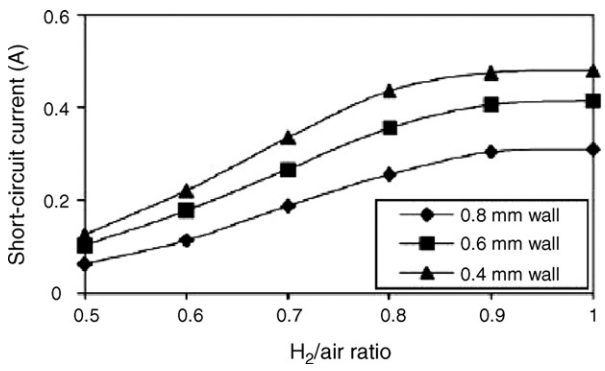

Fig. 30. Short-circuit current under different H_2/air ratio at flow rate of 12 m s^{-1} [32].

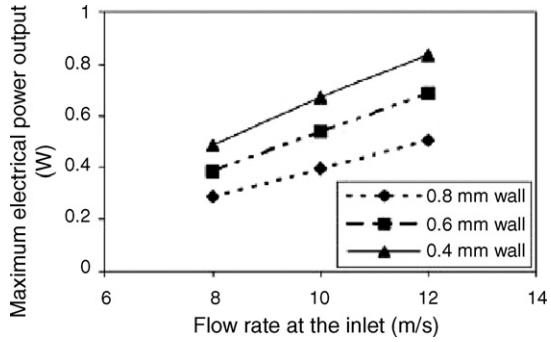

Fig. 31. Maximum electrical output under different flow rate at H_2/air ratio of 0.9 [32].

electrical power output increases drastically due to the increase of temperature along the wall. The increase is more significant in terms of absolute value when flow rate is high. In this experiment, Yang et al. [32] demonstrated that when the flow rate of hydrogen is 4.20 g h^{-1} and H_2/air ratio is 0.9, the maximum electrical power outputs that the micro-TPV system can produce are 0.92, 0.78 and 0.57 W for wall thickness of 0.4, 0.6 and 0.8 mm, respectively. The performance of the micro-TPV power generator with a wall thickness of 0.4 mm appears to be the best. However, the micro-TPV power generator with a wall thickness of 0.8 mm seems to perform the best.

4.5.3. Micro-combustor with and without backward facing step

Yang et al. [28] carried out an experiment to observe the effect of combustion in micro-cylindrical combustors with and without a backward facing step. This experiment involved the used of the micro-combustion experimental rig. The set-up is similar to the one that was used for the combustion studies described earlier in Section 4.5.1 (see Fig. 22). In this experiment, three different types of cylindrical micro-combustors were designed for testing. The design and specifications are illustrated in Fig. 33. For simplicity, all three micro-combustors are made of stainless steel.

Type 1 micro-combustor is a single cylindrical tube (see Fig. 33(1)). This is the simplest combustion structure. The combustion is expected to take place at the middle portion of the tube above the connector. Type 2 micro-combustor is a cylindrical tube with a backward facing step (see Fig. 33(2)). Type 3 micro-combustor is similar to Type 2 in structure but has a longer tube length after the step and a slight increase of the tube

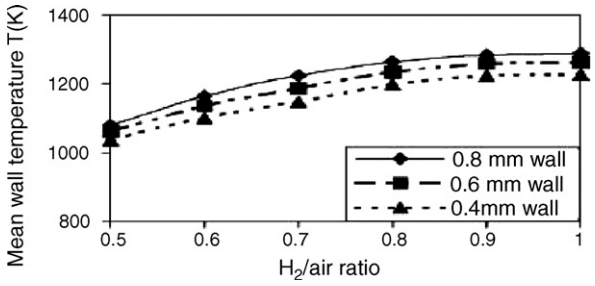

Fig. 32. Mean wall temperature under different H_2/air ratio [32].

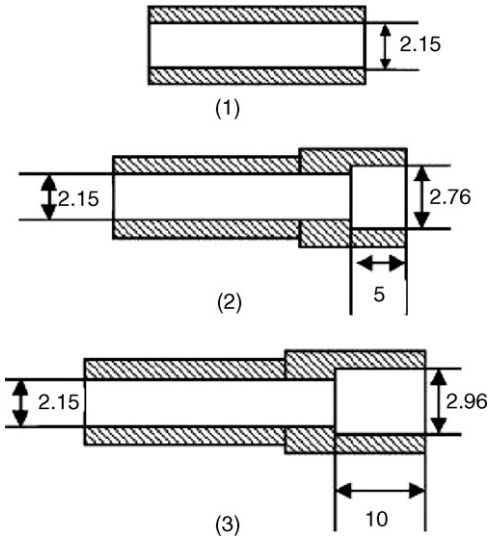

Fig. 33. Structures and dimensions of the three micro-combustors that were tested in the experiment [28]: (1) Type 1; (2) Type 2; (3) Type 3.

diameter (see Fig. 33(3)). As part of each tube is used for connection to the experimental rig (see Fig. 22), the length above the connector is 22.5 mm.

The major parameters that were measured in the experiment were the distribution of temperatures both along the outside wall of the micro-combustor and at the exit plane. This is because the wall temperature is a major factor reflecting the heat transported through the solid boundary. Compared to the total heat release during combustion, the heat transported becomes significantly large as the size of the combustor shrinks. The exhaust temperature provides an indication of whether combustion is complete [28]. For all three types of micro-combustor, different flow rates and H_2/air ratios were tested for the full range in which combustion could take place inside the combustion chamber. The results and observations for each micro-combustor (Type 1, Type 2 and Type 3) will be described in the following section.

4.5.3.1. Type 1 micro-combustor (straight tube). For the Type 1 micro-combustor, it was observed that combustion did not take place in the middle portion of the tube, but outside the tube, when flow speed exceeded 8 m s^{-1}. If the flow speed at the inlet dropped to 1.3 m s^{-1}, the flame extinguishes after a short-term combustion, which indicates that combustion could not be sustained at such a low flow rate. Furthermore, the position of the flame core moves with different inlet velocities. It is observed that with an increase in flow rate, a higher H_2/air ratio is required to achieve stable combustion in the combustor. Therefore, there are two major disadvantages with the Type 1 micro-combustor. The inlet velocity and H_2/air ratio to sustain a stable flame is constrained in a very narrow range and it is difficult to control the position of the flame.

4.5.3.2. Type 2 micro-combustor (backward facing step). The Type 2 micro-combustor is designed with a backward facing step in order to overcome the problems and disadvantages that were encountered with Type 1 micro-combustor. The distribu-

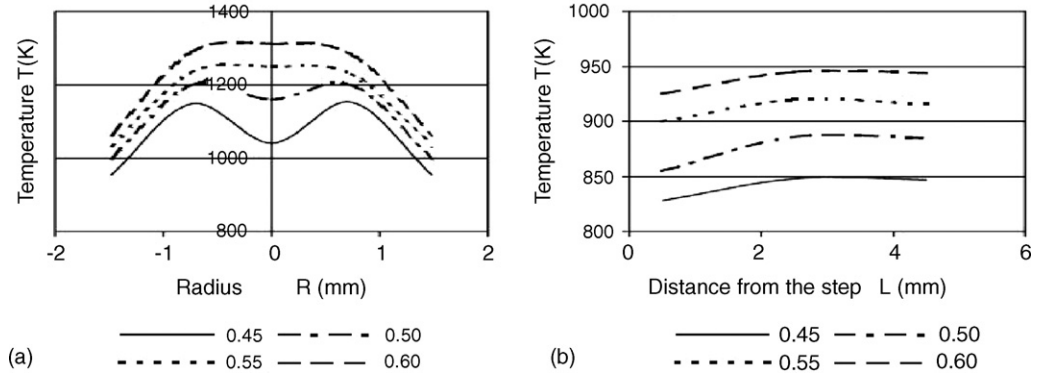

Fig. 34. The distribution of temperature for Type 2 micro-combustor at $V_{in} = 4\,m\,s^{-1}$, flow rate = 0.45–0.60: (a) at the exit plane and (b) along the wall [28].

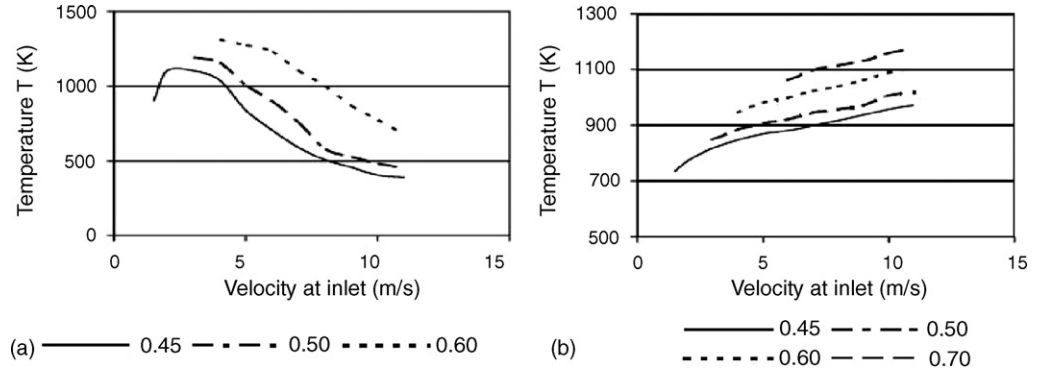

Fig. 35. Effect of inlet flow velocity and H_2/air ratio on temperature for Type 2 micro-combustor: (a) at the central line of exit and (b) average temperature along the wall [28].

tion of temperature on the exit plane and along the wall of Type 2 micro-combustor was observed when the inlet flow velocity is at $4\,m\,s^{-1}$. The result is shown in the plot in Fig. 34.

As the flow rate at the inlet is constant, with an increase in H_2/air ratio, both the temperatures at the outlet and along the wall increase drastically. Meanwhile, the position of peak temperature on the wall also moves slightly from the location near the exit towards the backward facing step. The temperature along the wall is almost uniform and the variation is less than 5%.

In terms of flow rate, when the flow rate is low, the total energy released from the combustion is small, so temperatures at exit and along the wall are low. With an increase in flow rate, the temperatures rise. But as flow rate increases further, the residence time of the fuel mixture in the combustor decreases, which leads to incomplete combustion for a large amount of the fuel mixture. As a result, the temperature at exit decreases. The effects of flow velocity on temperature distribution at exit and along the wall are illustrated in Fig. 35.

4.5.3.3. Type 3 micro-combustor (backward facing step). For the design of Type 3 micro-combustor, the distance from the backward facing step was doubled from 5 to 10 mm compared to Type 2 micro-combustor in order to further improve the efficiency of the combustion. The distribution of temperatures at exit and along the wall of the combustor at the inlet velocity of $4\,m\,s^{-1}$ is shown in Fig. 36.

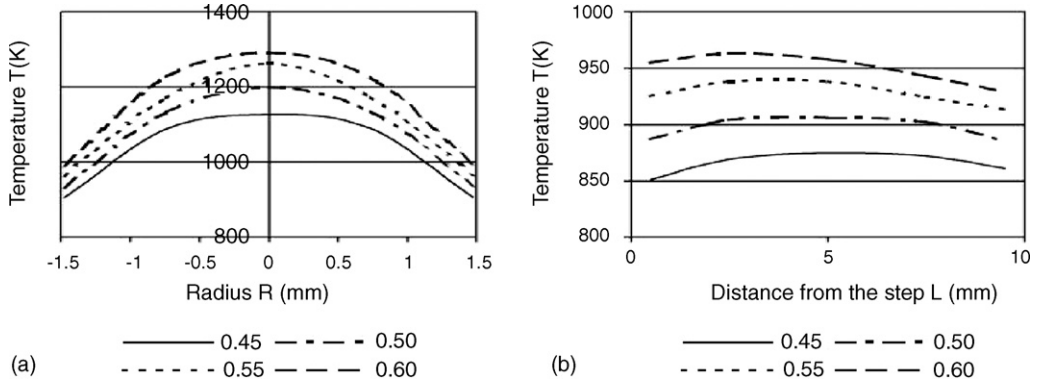

Fig. 36. The distribution of temperature for Type 3 micro-combustor at $V_{in} = 4\,m\,s^{-1}$, flow rate = 0.45–0.60: (a) at the exit plane and (b) along the wall [28].

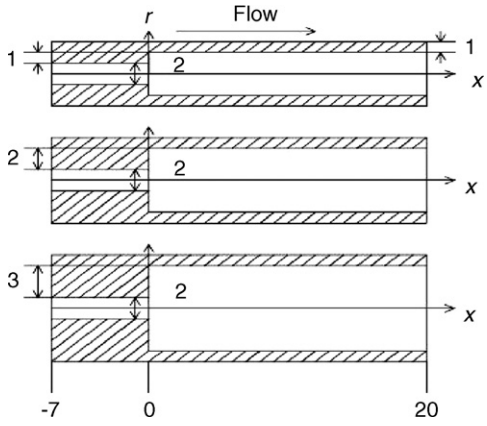

Fig. 37. Structures and dimensions of the three micro-combustors that were tested in the experiment [33].

Comparing Fig. 36 to Fig. 34, we can see that the main difference is that for Type 3 micro-combustor, the peak temperature occurs at the centre of the exit plane, whereas the peak temperature occurs at the side for Type 2 micro-combustor. This strongly indicates that the completeness of the combustion has been significantly improved [28].

4.5.3.4. Conclusion of backward facing step results. A backward facing step was designed to enhance the mixing process of the fuel mixture, and prolong the residence time. The results of the experiment done by Yang et al. [28] indicate that the micro-combustors with a backward facing step are very effective in controlling the position of the flame and widening the range of operation based on the inlet flow velocity and H_2/air ratio. The analysis on the pattern of the temperature distribution at the exit plane and along the wall suggests that the scenario of the combustion can be described in two steps: (1) the combustion near the wall due to the backward facing step, and (2) the combustion at the central region near the exit, which is induced by the hot products near the wall. As a result, a high (>1000 K) and uniform temperature along the wall of the combustor can be achieved. Therefore, the results indicate that the cylindrical micro-combustor with a backward facing step is adequate for the application of micro-TPV system [28].

4.5.4. Effects of step height of the micro-combustor

The earlier experimental studies on the effect of micro-combustors with and without a backward facing step (Section 4.5.3) have shown that micro-combustor with a sudden expan-

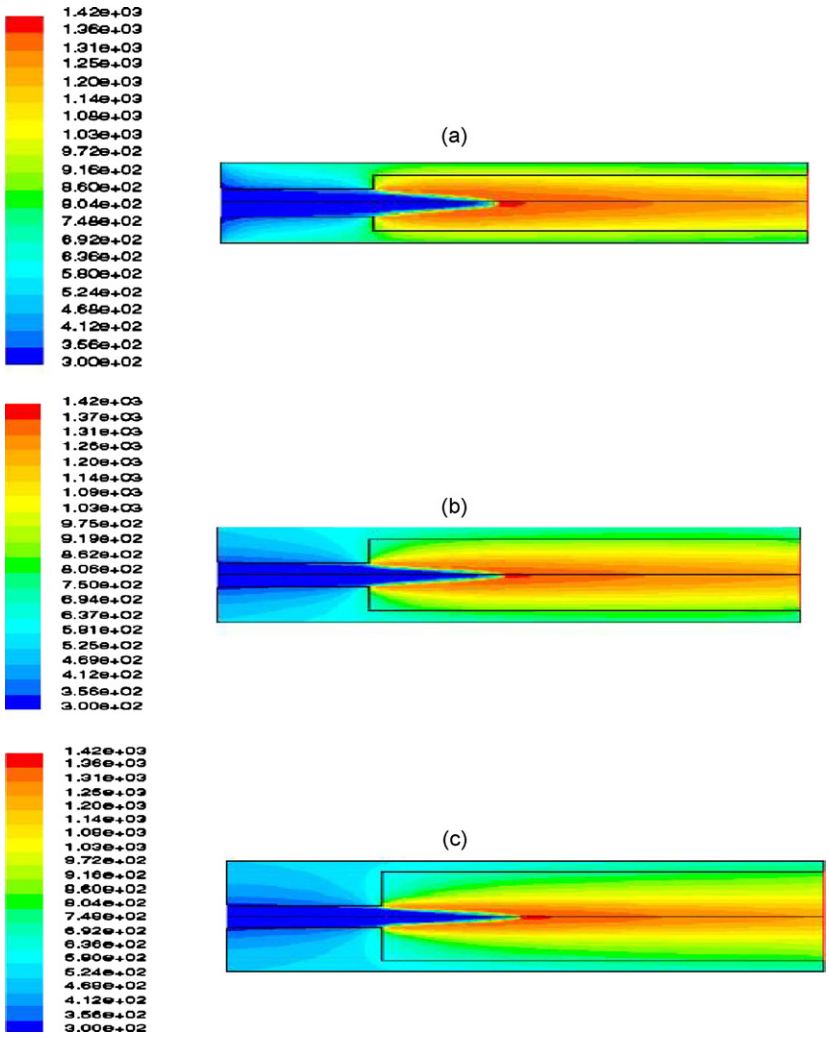

Fig. 38. Simulated temperature contours [33]: (a) for 1 mm step height; (b) for 2 mm step height; (c) for 3 mm step height.

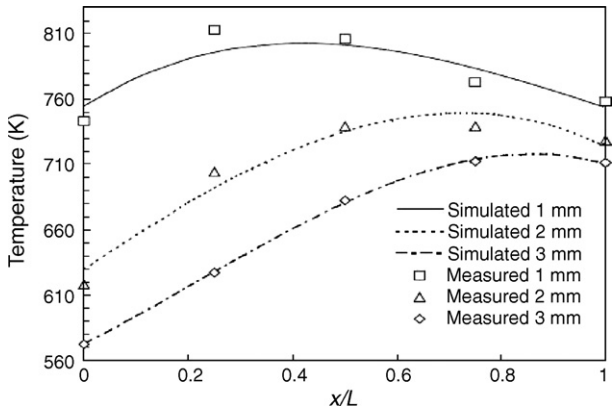

Fig. 39. Simulated and measured external wall temperature for different step heights [33].

sion step is advantageous for the application of the micro-TPV system. However, the effects of step height on the external wall temperature of the micro-combustor have not been well understood. Yang and co-workers [33] from the National University of Singapore carried out an experiment to investigate the effects of step height on the wall temperature of a micro-combustor. This experiment involved the used of the micro-combustion experimental rig. The set-up is similar to the one that was used for the combustion studies described earlier in Section 4.5.1 (see Fig. 22). In this experiment, three different types of cylindrical micro-combustors with different step heights of 1, 2 and 3 mm, respectively, were designed for testing. The specifications of the micro-combustors are illustrated in Fig. 37.

The experiment was conducted using each of the three vertical cylindrical micro-combustors, having the same geometry, the same inlet velocity and the same fuel–air ratio (the only difference is the step height). The fuel mixture is ignited at the exit plane of the micro-combustor. A stable flame can be established inside the tube by adjusting the flow rate or fuel–air ratio. The resulted flame and wall temperature are captured by thermocouples placed at the external wall surface and the exit plane, and indicated by the glow of the tube.

At the same time, a numerical simulation study is also carried out employing a H_2/air fuel mixture and the detailed reaction mechanism. Fig. 38 shows the plots of the temperature contour for the micro-combustors with the different step heights (1, 2 and 3 mm).

Fig. 39 shows the measured external wall temperature distribution from the experiment in the axial direction at the average inlet velocity of 4 m s^{-1} and the H_2/air ratio of 0.5. The simulation results are also plotted on this figure for comparison. Both experiment and simulation show that the external wall temperature increases with decreasing step height. The maximum difference between the measured and simulated external wall temperature is about 4% [33].

4.5.4.1. Conclusion of step height results. For both the measured and numerical simulation, the results show that the external wall temperature increases drastically with decreasing step height. However, the axial flame temperature is unaffected. Good agreement between the simulated and measured external wall temperature has been obtained. Using the external wall temperature measured at the constant inlet velocity and H_2/air ratio, Yang and co-workers [33] has demonstrated that emissive power increases with decreasing step height. At an average inlet velocity of 4 m s^{-1} and a H_2/air ratio of 0.5, emissive power of 6.6, 6.4 and 6.2 W has been achieved for the micro-combustors having step heights of 1, 2 and 3 mm, respectively [33]. As such, a 1 mm step height has been chosen in this case to incorporate into the design of the micro-TPV power device.

4.6. Summary of investigation results

A variety of investigations, numerical simulations, as well as experimental studies were conducted by Chou et al. [28,31–33,38] from the National University of Singapore on various aspects of the design of the micro-TPV device concerning the micro-combustor and SiC emitter. These experimental studies and investigations have been reviewed in this report and the results are summarised as follows:

- Increasing both the H_2/air ratio as well as flow rate will consequently lead to an increase in overall electric power output of the micro-TPV system [30,31].
- With the decrease in wall thickness of the micro-combustor, both the maximum electrical power output and short-circuit current increases drastically due to the increase of temperature along the wall [32].
- Backward facing step in micro-combustors provides a simple yet effective solution to enhance the mixing of fuel mixture and prolong the residence time. In addition, the step is very effective in controlling the position of the flame and widening the range of operation based on the inlet flow velocity and H_2/air ratio [28].
- The emissive power as well as external wall temperature of the micro-combustor increases drastically with decreasing step height [33].

5. Efficiency improvements for a micro-TPV device

5.1. Introduction

Just like any other micropower generators that are being developed around the world, the efficiency of the micro-TPV power generator that is being reviewed in this report is still low in the present design. There are still a lot of works that can be done before it can be establish for applications. As mentioned in Section 3.3, the overall efficiency of a conventional thermophotovoltaic (TPV) system is the product of the efficiencies of the PV cells, an optional filter, and the radiation source, consisting of the burner and the emitter, as follows:

$$\eta_{\text{overall}} = \eta_{\text{emitter}} \times \eta_{\text{filter}} \times \eta_{\text{PV}}$$

5.2. Efficiency of micro-combustor (SiC emitter) and overall efficiency

In the current design of the micro-TPV power generator reviewed in this report, silicon carbide (SiC) is being chosen as

the material for the emitter and gallium antimonide (GaSb) for the PV cells. The micro-combustor is able to achieve an average temperature of 1325 K along the wall, and the biggest temperature difference is less than 5% when the H_2 flow rate is 4.20 g h^{-1} (1.167×10^{-6} kg s^{-1}) and the H_2/air ratio is 0.9. Thus, according to Planck's rule, the spectral distribution of emissive power of the SiC emitter (modeled as a blackbody emitter) is

$$\text{Planck's law}: \quad W_b(\lambda, T) = \frac{C_1}{\lambda^5(e^{C_2/\lambda T} - 1)}$$

where $C_1 = 2\pi hc^2 = 3.742 \times 10^{-4}$ W μm^4 m^{-2} and $C_2 = hc/k = 1.439 \times 10^4$ μm K.

Thus, the total emissive power of the SiC emitter is

$$\int_0^\infty W_b(\lambda, T) = \int_0^\infty \frac{C_1}{\lambda^5(e^{C_2/\lambda T} - 1)} d\lambda = \sigma T^4$$
$$= (5.670 \times 10^{-8}) \times 1325^4 = 174.761 \times 10^3 \text{ W m}^{-2}$$

where σ is the Stefan–Boltzmann constant (5.670×10^{-8} W m^{-2} K^{-4}).

In the above calculation C_1 and C_2 are Planck's first and second constant, respectively, h is Planck's constant (6.63×10^{-34} J s), c is the speed of light (2.998×10^8 m s^{-1}), and T is the temperature of the SiC emitter (1325 K). The emissive surface (S_E) of the micro-combustor is

$$S_E = 2\pi r \times L = 2\pi(1.9 \text{ mm}) \times (16 \text{ mm})$$
$$= 1.91 \times 10^{-4} \text{ m}^2 (1.91 \text{ cm}^2)$$

Thus, the efficiency of the micro-combustor (SiC emitter) can be calculated by

$$\therefore \eta_{\text{emitter}}(\text{SiC}) = \frac{P_{\text{rad}}}{H_{\text{fuel}}\dot{m}} = \frac{\int_0^\infty W_b(\lambda, T)\varepsilon_{\text{SiC}} S_E \, d\lambda}{H_{\text{fuel}}\dot{m}} = \frac{\sigma T^4 \varepsilon_{\text{SiC}} S_E}{H_{\text{fuel}}\dot{m}}$$
$$= \frac{(174.761 \times 10^3 \text{ W m}^{-2})(0.9)(1.91 \times 10^{-4} \text{ m}^{-2})}{(120.1 \text{ MJ kg}^{-1})(1.167 \times 10^{-6} \text{ kg s}^{-1})}$$
$$= 0.214 = 21.4\%$$

where P_{rad} is the net radiation power emitted by the emitter and H_{fuel} is the heating value of fuel (we use $\text{LHV}_{\text{hydrogen}}$ = 120.1 MJ kg^{-1}).

The micro-TPV power generator is reported to produce 0.92 W of electrical power as mentioned in Section 4. The efficiency of the GaSb PV cell with filter is 3.08% (~2.64% without filter). Thus, the overall efficiency (η_{overall}) of the micro-TPV power generator is

$$\therefore \eta_{\text{overall}} = \frac{\text{Electrical\_Power\_Output}}{H_{\text{fuel}}\dot{m}} = \frac{0.92 \text{ W}}{(120.1 \text{ MJ kg}^{-1})(1.167 \times 10^{-6} \text{ kg s}^{-1})}$$
$$= 0.00656 = 0.66\%$$

Alternatively, we can find the overall efficiency by calculating:

$$\therefore \eta_{\text{overall}} = (\eta_{\text{PV}} \times \eta_{\text{filter}}) \times \eta_{\text{emitter}} = 0.0308 \times 0.214$$
$$= 0.00659 = 0.66\%$$

This efficiency is not very high. Therefore possible ways of improving it have been discussed in the following section.

5.3. Possible efficiency improvements

5.3.1. Replacing the material of the PV cells

In the present design of the micro-TPV power generator, GaSb PV cells are being used. GaSb cell has a band gap of 0.72 eV, corresponding to a wavelength of 1.7 μm. This may not be very ideal for optimum efficiency and can be improve if we can lower the band gap of the cells. Lowering the band gap of PV cells will allow more photons with lower energy to be absorbed by the PV cells and creates electron–hole pairs. This is because only photons radiated by the emitter having energy greater than the band gap of the PV cells can be converted into electricity. If the present GaSb (gallium antimonide) PV cells is replace with GaInAsSb (gallium indium arsenic antimonide) PV cells, the performance of the micro-TPV power generator can be further improved due to the lower band gap of the GaInAsSb PV cells [42]. In a paper written by Yang et al. [29], high quantum efficiency GaInAsSb PV cells were investigated and band gap as low as 0.5 eV can be obtained. The quantum efficiency for GaInAsSb PV cells (as a function of wavelength) is shown in Fig. 40.

If the GaInAsSb PV cells are incorporated into the micro-TPV power device, it will produce an efficiency of ~4.8% (~4.18% without filter) with the present micro-combustor and SiC emitter configurations. Therefore, the new overall efficiency can be calculated by

$$\therefore \eta_{\text{overall}} = (\eta_{\text{PV}} \times \eta_{\text{filter}}) \times \eta_{\text{emitter}} = 0.048 \times 0.214$$
$$= 0.0103 = 1.03\%$$

The electrical power output based on the above efficiency can be calculated as follows:

$$\eta_{\text{overall}} = \frac{\text{Electrical\_Power\_Output}}{H_{\text{fuel}}\dot{m}} = 0.0103$$

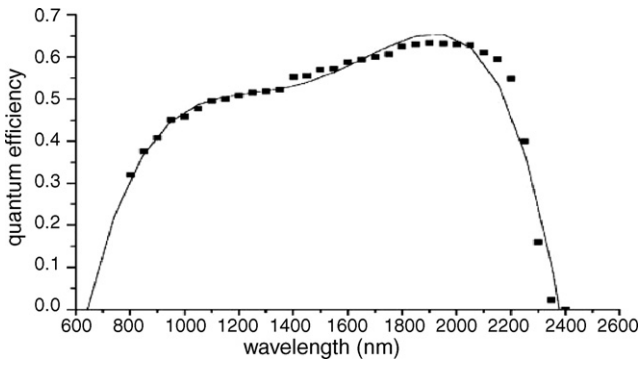

Fig. 40. Quantum efficiency of GaInAsSb PV cells [29].

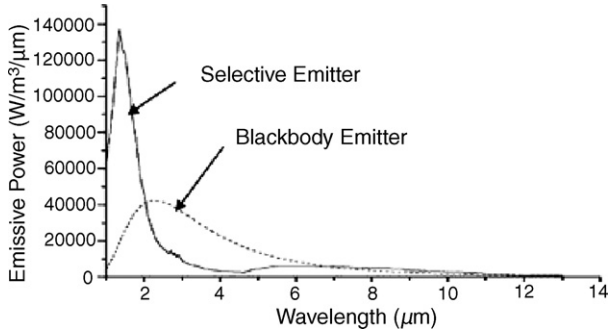

Fig. 41. Emissive power spectrum of selective emitter and blackbody emitter [37].

$\therefore$ Electrical_Power_Output = (120.1 MJ kg^{-1}) (1.167 × 10^{-6} kg s^{-1}) × 0.0103 = 1.45 W.

This will give a power output density of 0.78 W cm^{-2} (for the emissive area of 1.91 cm^2). Therefore, theoretically speaking, the micro-TPV power generator should be able to deliver an electrical power output of about 1.45 W, which was also predicted by Yang et al. [7], when the present GaSb PV cells are replace with GaInAsSb PV cells. However, the setback is that the GaSb PV cell is the only commercial PV cell available for TPV applications so far.

5.3.2. Replacing the material of the emitter

As mentioned earlier, the GaSb PV cell in the current design has a band gap of 0.72 eV, corresponding to a wavelength of 1.7 μm. This means that those emitted photons with wavelength longer than 1.7 μm cannot generate free electrons to produce electricity when impinge on the PV cells. Thus, if the emitter can be improved to emit more photons with shorter wavelength (<1.7 μm), the overall efficiency of the system will be improved as more photons will be able to be absorbed by the PV cells.

5.3.2.1. Replacing with Co/Ni-doped MgO emitter. In a paper by Ferguson and Dogan [37] a highly efficient thermally excited NiO-doped MgO matched emitter for TPV energy conversion was investigated. The emissive power spectrum is matched very efficiently to the response of GaSb PV cells. It has been shown that doping concentrations of 2–4 wt.% Co_3O_4 or NiO within a low infrared emissivity MgO host will produce matched emitters with continuous, strong radiant emissions in the optimal energy range between 1 and 2 μm and minimal radiation at non-convertible wavelengths. The emissive power of a selective emitter (Co/Ni-doped MgO) compared to a blackbody emitter (SiC emitter) is shown in Fig. 41.

Therefore, if we replace the current SiC emitter in the micro-TPV power generator to a Co/Ni-doped MgO emitter, it will be able to reshape the radiation spectrum, so that the radiation concentrates at shorter wavelengths where the quantum yield of infrared responding PV cells is highly efficient. This will thus affect the efficiency of the GaSb PV cells, which will consequently improve to ~15.72% [29] if the Co/Ni-doped MgO emitter is incorporated into the micro-TPV system instead of SiC emitter. This is due to the increase in the quantity of absorbable photons, leading to a higher generation of free electrons to produce electricity. With this, we can calculate the overall efficiency ($\eta_{overall}$) of the micro-TPV system, assuming that the efficiency of the Co/Ni-doped MgO emitter remains the same as the SiC emitter:

$$\therefore \eta_{overall} = (\eta_{PV} \times \eta_{filter}) \times \eta_{emitter} = 0.1572 \times 0.214$$
$$= 0.0336 = 3.36\%$$

The electrical power output based on the above efficiency can be calculated as follows:

$$\eta_{overall} = \frac{Electrical\_Power\_Output}{H_{fuel}\dot{m}} = 0.0336$$

$\therefore$ Electrical_Power_Output = (120.1 MJ kg^{-1}) (1.167 × 10^{-6} kg s^{-1}) × 0.0336 = 4.71 W.

This will give a power output density of 2.47 W cm^{-2} (for the emissive area of 1.91 cm^2). Therefore, theoretically speaking, the micro-TPV power generator should be able to deliver an electrical power output of about 4.71 W, when the present SiC emitter is replace with the thermally excited Co/Ni-doped MgO emitter.

5.3.2.2. Replacing with micro-structured tungsten emitter. In a paper by Ferber et al. [44], a promising new TPV concept based on micro-structured, infrared-selective tungsten emitters is analysed. Such emitters are well adapted to the spectral response of the GaSb PV cells. In a cylindrical emitter and cell geometry sample similar to the micro-TPV system reviewed in this report, the micro-structured tungsten emitter is able to raise the efficiency of the GaSb PV cells to the range of 14.9–15.5% depending on the side reflectance. Applying the micro-structured tungsten as selective emitter should consequently lead to a further increase in the overall efficiency of the micro-TPV system. However the concept is still relatively new and unproven.

5.3.3. Increasing the length of micro-combustor

Increasing the length of the micro-combustor will consequently lead to an increase in the emissive surface area. Also, the active area of the GaSb PV cell has to correspond with the surface area of the SiC emitter. In other words, if the length of the micro-combustor is increased, the active length of the GaSb PV cells will also have to be increased, due to the cylindrical geometry of the micro-TPV device. If the length of the combustor is increase from the present length of 16 to 22 mm (an increase of 6 mm), the new emissive surface area will become (assuming the wall thickness and diameter remain constant):

$$S_E = 2\pi r \times L = 2\pi(1.9\,mm) \times (22\,mm)$$
$$= 2.62 \times 10^{-4}\,m^2 (2.62\,cm^2)$$

With the increase in length, the temperature along the wall of the micro-combustor remains near uniform and is able to maintain the same temperature [34]. Thus, the efficiency of the

micro-combustor (SiC emitter) can be calculated by

$$\therefore \eta_{\text{emitter}}(\text{SiC}) = \frac{P_{\text{rad}}}{H_{\text{fuel}}\dot{m}} = \frac{\int_0^\infty W_b(\lambda, T)\varepsilon_{\text{SiC}} S_E \, d\lambda}{H_{\text{fuel}}\dot{m}} = \frac{\sigma T^4 \varepsilon_{\text{SiC}} S_E}{H_{\text{fuel}}\dot{m}}$$
$$= \frac{(174.761 \times 10^3 \, \text{W m}^{-2})(0.9)(2.62 \times 10^{-4} \, \text{m}^2)}{(120.1 \, \text{MJ kg}^{-1})(1.167 \times 10^{-6} \, \text{kg s}^{-1})}$$
$$= 0.294 = 29.4\%$$

As mentioned, if the length of the micro-combustor is increased, the active length of the GaSb PV cells will also have to be increased (from 15.5 to 22 mm). This will lead to an increase in the efficiency of the GaSb PV cells (~3.52%) since the area is larger now. Therefore, the new overall efficiency (η_{overall}) can be calculated by

$$\therefore \eta_{\text{overall}} = (\eta_{\text{PV}} \times \eta_{\text{filter}}) \times \eta_{\text{emitter}}$$
$$= 0.0352 \times 0.294 = 0.0103 = 1.03\%$$

The electrical power output based on the above efficiency can be calculated as follows:

$$\eta_{\text{overall}} = \frac{\text{Electrical\_Power\_Output}}{H_{\text{fuel}}\dot{m}} = 0.0103$$

$\therefore$ Electrical_Power_Output = $(120.1 \, \text{MJ kg}^{-1})$ $(1.167 \times 10^{-6} \, \text{kg s}^{-1}) \times 0.0103 = 1.45$ W.

This will give a power output density of $0.55 \, \text{W cm}^{-2}$ (for the emissive area of $2.62 \, \text{cm}^2$), which is actually lower than the original design (which also justifies the cubic-square law—see Section 2.2.1). Therefore, theoretically speaking, the micro-TPV power generator should be able to deliver an electrical power output of about 1.45 W, which was also predicted by Yang et al. [34], when the present micro-combustor length is increased from 16 to 22 mm.

5.3.4. Increasing other physical dimensions of micro-combustor

Increasing any other physical dimensions of the micro-combustor will consequently lead to an increase in the emissive surface area (S_E). As mentioned, the efficiency of the SiC emitter (micro-combustor) is given by the following formula:

$$\therefore \eta_{\text{emitter}}(\text{SiC}) = \frac{P_{\text{rad}}}{H_{\text{fuel}}\dot{m}} = \frac{\int_0^\infty W_b(\lambda, T)\varepsilon_{\text{SiC}} S_E \, d\lambda}{H_{\text{fuel}}\dot{m}} = \frac{\sigma T^4 \varepsilon_{\text{SiC}} S_E}{H_{\text{fuel}}\dot{m}}$$

Therefore, based on the above formula, we can see that the larger the emissive surface area (S_E), the higher the efficiency of the SiC emitter (micro-combustor). This will subsequently lead to a higher overall efficiency of the micro-TPV system. It should however be mentioned that this is only possible if the wall temperature and distribution can be kept constant despite the changes to the physical dimensions of the micro-combustor. For example, changing certain specifications such as the wall thickness may affect the temperature of the micro-combustor (as seen in the review in Section 4). It is also worth noticing that as the surface area increases, the power output density will decrease.

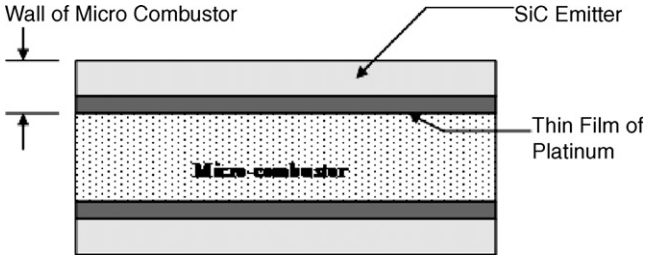

Fig. 42. Thin film of platinum can be deposited on the inner surface of the micro-SiC combustor to act as a catalyst.

5.3.5. Employing a catalytic combustion

Improvement can also be made to the micro-TPV system by employing a catalytic combustion. A catalytic combustion can increase the temperature along the wall of the micro-combustor drastically. In an experimental study done by Yang et al. [38], platinum was tested as a material for the selective emitter. The results indicate that platinum can significantly improve flame structure in the micro-cylindrical combustor, and increase the wall temperature by about 230 K as compared to the SiC emitter, which is critical to the overall efficiency of the micro-TPV device. However, the drawback is that the emissivity of platinum is too low at short wavelengths (emissivity of platinum is only about 0.06–0.18), which will restrict the radiation of photons.

However, if a thin film of platinum can be deposited on the inner surface of the micro-SiC combustor to act as a catalyst as illustrated in Fig. 42, the emissivity of the emitter surface can still be maintained, and at the same time, increased the temperature of the wall micro-combustor. With such configuration, the wall temperature could be increased to about 1555 K (increase by 230 K).

Thus, the new efficiency of the micro-combustor (SiC emitter) with the incorporation of a thin film of platinum on the inner surface can be calculated by

$$\therefore \eta_{\text{emitter}}(\text{SiC}) = \frac{P_{\text{rad}}}{H_{\text{fuel}}\dot{m}} = \frac{\int_0^\infty W_b(\lambda, T)\varepsilon_{\text{SiC}} S_E \, d\lambda}{H_{\text{fuel}}\dot{m}} = \frac{\sigma T^4 \varepsilon_{\text{SiC}} S_E}{H_{\text{fuel}}\dot{m}}$$
$$= \frac{(5.67 \times 10^{-8} \, \text{W m}^{-2} \, \text{K}^{-4})(1555 \, \text{K})^4 (0.9)(1.91 \times 10^{-4} \, \text{m}^2)}{(120.1 \, \text{MJ kg}^{-1})(1.167 \times 10^{-6} \, \text{kg s}^{-1})}$$
$$= 0.407 = 40.7\%$$

The efficiency of the GaSb PV cells will also increase as a result. This is because the higher wall temperature of the micro-combustor has improve the distribution of spectral, resulting in producing a larger portion of photons having energy greater than that of the PV cells (0.72 eV). The efficiency of the GaSb PV cells could be improve to an estimation of ~6.16%.

Table 2
System efficiency and power output on different configurations

Micro-TPV device Configuration	Power output density ($W\,cm^{-2}$)	Predicted electrical power output (W)	Predicted efficiency of emitter (micro-combustor), $\eta_{emitter}$ (%)	Predicted efficiency of PV cells, η_{PV} (%)	Overall efficiency, $\eta_{overall}$ (%)
SiC emitter, GaSb PV cells	0.48	**0.92**	21.4	3.08	**0.66**
SiC emitter, GaInAsSb PV cells	0.78	**1.45**	21.4	4.80	**1.03**
Co/Ni-doped MgO matched emitter, GaSb PV cells	2.47	**4.71**	21.4	15.72	**3.36**
SiC emitter, GaSb PV cells, length increased to 22 mm	0.55	**1.45**	29.4	3.52	**1.03**
SiC emitter, GaSb PV cells, platinum as catalyst	1.84	**3.51**	40.7	6.16	**2.51**
Co/Ni-doped MgO matched emitter, GaSb PV cells, length increased to 22 mm	2.10	**5.5**	29.4	13.3	**3.92**

Therefore, the new overall efficiency ($\eta_{overall}$) of the system can be calculated by

$$\therefore \eta_{overall} = (\eta_{PV} \times \eta_{filter}) \times \eta_{emitter} = 0.0616 \times 0.407 = 0.0251 = 2.51\%$$

The electrical power output based on the above efficiency can be calculated as follows:

$$\eta_{overall} = \frac{Electrical\_Power\_Output}{H_{fuel}\dot{m}} = 0.0251$$

$\therefore$ Electrical_Power_Output = $(120.1\,MJ\,kg^{-1})$ $(1.167 \times 10^{-6}\,kg\,s^{-1}) \times 0.0251 = 3.51\,W$.

This will give a power output density of $1.84\,W\,cm^{-2}$ (for the emissive area of $1.91\,cm^2$). Therefore, theoretically speaking, the micro-TPV power generator should be able to deliver an electrical power output of about 3.51 W, when a thin film of platinum is deposited on the inner surface of the micro-SiC combustor to act as a catalyst.

5.3.6. Replacing with Co/Ni-doped MgO emitter and increasing length

As discussed in Section 5.3.3 earlier, increasing the length of the micro-combustor from 16 to 22 mm will result in an emissive surface area of $2.62 \times 10^{-4}\,m^2$ ($2.62\,cm^2$). If we implement this configuration and at the same time replace the SiC emitter with the thermally excited Co/Ni-doped MgO matched emitter, the power output of the micro-TPV system will increase greatly. Yang et al. [34] predicted that with such a configuration, an electrical output of 5.5 W can be expected. This is by far the highest power output predicted among all the possible improvements investigated so far. The overall efficiency ($\eta_{overall}$) for this configuration can be calculated as follows:

$$\therefore \eta_{overall} = \frac{Electrical\_Power\_Output}{H_{fuel}\dot{m}} = \frac{5.5\,W}{(120.1\,MJ\,kg^{-1})(1.167 \times 10^{-6}\,kg\,s^{-1})} = 0.0392 = 3.92\%$$

This will give a power output density of $2.10\,W\,cm^{-2}$ (for the emissive area of $2.62\,cm^2$).

5.4. Summary of the possible efficiency improvements

The efficiency of the micro-combustor (emitter) as well as the overall efficiency of the micro-TPV power device has been investigated in this section. Assumptions and calculations were made to predict the efficiencies based on various changes made to the device such as replacing the material of the emitter and PV cells, altering the physical dimensions, as well as introducing a catalytic combustion. Table 2 summarises the predicted efficiencies as well as the electrical power output of the micro-TPV power device based on different system configurations. From Table 2, it can be observed that the electrical power output and efficiency of the micro-TPV system with GaInAsSb cells are about 1.5 times that with GaSb cells (when SiC is being used as the material for the emitter). However, when the emitter is made of Co/Ni-doped MgO materials (with GaSb PV cells), both the electrical power output and efficiency of the system are much higher. Likewise, when a thin film of platinum is deposited on the inner surface of the micro-SiC combustor to act as a catalyst, both the electrical power output and efficiency of the system also improved significantly. These results indicated that the choice of materials for the emitter is very significant in improving the performance of micro-TPV systems, as compared to the material for PV cells.

6. Conclusions and recommendations

6.1. Conclusions

A detailed review is carried out on the current micropower technology. In particular, a prototype micropower device based on the concept of thermophotovoltaic (TPV) system of generating electricity is being reviewed for improvement. This prototype micro-TPV power generator [7] is currently under research and development by the National University of Singapore (NUS). The system is made up of a micro-cylindrical SiC combustor, a simple nine-layer dielectric filter and a GaSb

photovoltaic (PV) cell array. When the flow rate of hydrogen is $4.20\,g\,h^{-1}$ and H_2/air ratio is 0.9, the system is able to deliver an electric power output of 0.92 W in a micro-combustor of $0.113\,cm^3$ in volume. The overall efficiency is 0.66%.

The individual components of the micro-TPV power device have performed well, but there have not been enough works to demonstrate its competency for commercial applications just yet. In this report, focus is given on the possible improvements to the micro-TPV power device, in particularly the efficiency of the micro-combustor, PV cells, and consequently the overall efficiency. Just like any other micropower generators that are being developed around the world, the efficiency of the reviewed micro-TPV device is still low in the present design.

Assumptions and calculations were made to predict possible higher efficiencies based on various changes made to the device such as replacing the materials of the emitter and PV cells, altering the physical dimensions, as well as introducing a catalytic combustion. It is observed that the electrical power output and efficiency of the micro-TPV system with GaInAsSb cells are about 1.5 times that with GaSb cells (when SiC is being used as the material for the emitter). However, when the emitter is made of Co/Ni-doped MgO materials (with GaSb PV cells), both the electrical power output and efficiency of the system are much higher. Likewise, when a thin film of platinum is deposited on the inner surface of the micro-SiC combustor to act as a catalyst, both the electrical power output and efficiency of the system also improved significantly. These results indicated that the choice of materials for the emitter is very significant in improving the performance of micro-TPV systems, as compared to the material for PV cells.

Therefore, we conclude that priority should be given to the choice of materials for the emitter (wall of micro-combustor) in the design and construction of a micro-TPV power device. The most suitable material for the emitter will significantly enhance the electrical power output of the device, and consequently produce a higher overall efficiency.

The highest predicted electrical power output is 5.5 W with an overall efficiency of 3.92%. In the configuration, the SiC emitter is replaced with a thermally excited Co/Ni-doped MgO matched emitter, and the length of the micro-combustor is increased from 16 to 22 mm (to give an emissive surface area of $2.62\,cm^2$). GaSb PV cells are being used.

6.2. Future work

The design of the micro-TPV power generator reviewed in this report is still very much in its development stage. There are still a lot of works that can be done before it can be established for commercial applications. There are still many possibilities for improvement. Some of the recommended future works that can be carried out are listed below:

- There are still many other issues to consider in predicting the efficiencies of the micro-TPV power device, including: non-uniformity of photon flux, photon loss mechanisms, micro-combustor temperature, as well as mismatched performances of individual cells [45]. These factors are difficult to model. Future research could be done on these areas.
- Experimental studies could be carried out in future to further ascertain the accuracy of the improved efficiencies discussed in Section 5.
- Further optimise the micro-combustor both by numerical simulation and experimental studies. This will lead to further improvement of the micro-TPV system.
- Develop new micro-combustor that can achieve stable combustion and high wall temperature. This will enhance the emitting power and thus improve the overall efficiency.
- Further research could be done to develop a proper selective emitter to improve the efficiency of the micro-combustor and consequently the performance of the micro-TPV system. Likewise, we can further improve the efficiency of the available PV cells.
- Investigate the possibility of integrating the TPV system with a gas turbine to recover the exhaust heat, so that the efficiency could be further enhanced.

Acknowledgement

The project is supported by the University of Queensland.

References

[1] W.M. Yang, S.K. Chou, C. Shu, A.W. Li, H. Xue, Int. J. Comput. Eng. Sci. 4 (2003) 481–484.
[2] A.H. Epstein, S.D. Senturia, G. Anathasuresh, et al., Proceedings of the Ninth International Conference on Solid-State Sensors and Actuators, Chicago, IL, June, 1997.
[3] A. Mehra, X. Zhang, A.A. Ayon, I.A. Waitz, M.A. Schmidt, C.M. Spadaccini, J. Microelectromech. Syst. 9 (2000) 517–527.
[4] K. Fu, A.J. Knobloch, B.A. Cooley, D.C. Walther, A.C. Fernandez-Pello, D. Liepmann, K. Miyaska, Proceedings of the National Heat Transfer Conference 2001, Anaheim, CA, June 10–12, 2001, pp. 1–6.
[5] L. Sitzki, K. Borer, E. Schuster, P.D. Ronney, Proceedings of the Third Asia-Pacific Conference on Combustion, Seoul, Korea, June 24–27, 2001.
[6] S.J. Lee, A. Chang-Chien, S.W. Cha, R. O'Hayre, Y.I. Park, Y. Saito, F.B. Prinz, J. Power Sources 112 (2002) 410–418.
[7] W.M. Yang, S.K. Chou, C. Shu, H. Xue, Z.W. Li, J. Phys. D: Appl. Phys. 37 (2004) 1017–1020.
[8] D. Linden, Handbook of Batteries, McGraw-Hill, New York, 2002.
[9] C.K. Dyer, J. Power Sources 106 (2002) 31–34.
[10] Energizer Holdings, Inc., 2005, http://www.energizer.com/.
[11] P.D. Ronney, http://carambola.usc.edu/Research/MicroFIRE/.
[12] A.C. Fernandez-Pello, Proc. Combust. Inst. 29 (2002) 883–898.
[13] D.C. Kyritsis, S. Roychoudhury, C.S. McEnally, L.D. Pfefferle, A. Gomez, Exp. Thermal Fluid Sci. 28 (2003) 763–770.
[14] S.A. Jacobson, A.H. Epstein, Proceedings of the International Symposium on Micro-mechanical Engineering, December 1–3, 2003.
[15] W. Yang, Proceedings of the 28th International Symposium on Combustion, Edinburgh, UK, 30 July–4 August, 2000, pp. 1–4.
[16] A.P. Pisano, A.C. Fernandez-Pello, MEMS rotary internal combustion engine, http://www.me.berkeley.edu/mrcl/index.html.
[17] R. Decher, Direct Energy Conversion: Fundamentals of Electric Power Production, Oxford University Press, New York, 1997.
[18] S. Stevens, J. Driesen, R. Belmans, A Brief Overview of Power Generating Micro Electromechanical Systems, ESAT, div. ELECTA, K.U. Leuven, 2002.
[19] C. Shearwood, R. Yates, Electron. Lett. 33 (1997) 1883–1884.
[20] Paul Scherrer Institute, Laboratory for micro- and nanotechnology: thermophotovoltaics, 2004, http://lmn.web.psi.ch/shine/tpv1.htm.

[21] W. Yang, S.K. Chou, C. Shu, H. Xue, Z. Li, Appl. Phys. Lett. 84 (2004) 3864–3866.
[22] F. Ochoa, C. Eastwood, P.D Ronney, B. Dunn, Proceedings of the Seventh International Microgravity Combustion Workshop, Cleveland, OH, June, 2003.
[23] D.C. White, R.D. Wedlock, J. Blair, The 15th Annual Proceedings, Power Sources Conference, May, 1961, pp. 125–132.
[24] D.C. White, H.C. Hottel, Proceedings of the First NREL Conference on Thermophotovoltaic Generation of Electricity, CO, USA, 1995, p. 425.
[25] H. Sai, Y. Kanamori, H. Yugami, PowerMEMS 2003 International Workshop, December, 2003, pp. 118–121.
[26] Z. Chen, P.L. Adair, M.F. Rose, Proceedings of the 31st Intersociety Energy Conversion Engineering Conference, Part 2 (of 4), Washington, DC, USA, August 11–16, 1996, pp. 1013–1017.
[27] A. Catalano, Thermophotovoltaics: A New Paradigm for Power Generation? National Renewable Energy Laboratory, 1996, pp. 495–499.
[28] W. Yang, S.K. Chou, C. Shu, Z.W. Li, H. Xue, Appl. Thermal Eng. 22 (2002) 1777–1787.
[29] W.M. Yang, S.K. Chou, C. Shu, Z.W. Li, H. Xue, Sol. Energy Mater. Sol. Cells 80 (2003) 95–104.
[30] H. Xue, W.M. Yang, S.K. Chou, C. Shu, Z. Li, Microscale Thermophys. Eng. 9 (2005) 85–97.
[31] W.M. Yang, S.K. Chou, C. Shu, H. Xue, Z.W. Li, J.F. Pan, Energy Convers. Manage. 44 (2003) 2625–2634.
[32] W.M. Yang, S.K. Chou, C. Shu, H. Xue, Z.W. Li, Sens. Actuators A 119 (2004) 441–445.
[33] Z.W. Li, S.K. Chou, C. Shu, W.M. Yang, J. Micromech. Microeng. 15 (2004) 207–212.
[34] W.M. Yang, S.K. Chou, C. Shu, H. Xue, Z.W. Li, J. Microelectromech. Syst. 13 (2004) 851–855.
[35] M.G. Krishna, M. Rajendran, D.R. Pyke, A.K. Bhattacharya, Sol. Energy Mater. Sol. Cells 59 (1999) 337–347.
[36] A. Heinzel, V. Boerner, V. Gombert, V. Wittwer, J. Luther, Proceedings of the Thermophotovoltaic Generation of Electricity 4th NREL Conference, Denver, CO, 1999, pp. 191–196.
[37] L.G. Ferguson, F. Dogan, Mater. Sci. Eng. B 83 (2001) 35–41.
[38] W.M. Yang, S.K. Chou, C. Shu, H. Xue, Z.W. Li, J. Micromech. Microeng. 15 (2005) S239–S242.
[39] JX Crystals, Inc., The JXC Specialty—Broadband, High Power Density PhotoVoltaics, 2005, http://www.jxcrystals.com/.
[40] L.G. Ferguson, L.M. Fraas, Sol. Energy Mater. Sol. Cells 39 (1995) 11–18.
[41] M.W. Wanlass, J.S. Ward, K.A. Emery, M.M. Al-Jassim, K.M. Jones, T.J. Coutts, Sol. Energy Mater. Sol. Cells 41 (1996) 405–417.
[42] C.A. Wang, H.K. Choi, S.L. Ransom, G.W. Charache, L.R. Danielson, D.M. DePoy, Appl. Phys. Lett. 75 (1999) 1305–1307.
[43] L.M. Fraas, G.R. Girard, J.E. Avery, B.A. Arau, V.S. Sundaram, J.M. Gee, J. Appl. Phys. 66 (1989) 3866–3870.
[44] J. Ferber, J. Aschaber, C. Hebling, A. Heinzel, R. Wiehle, M. Zenker, J. Luther, Proceedings of the 16th European Photovoltaic Solar Energy Conference and Exhibition, Glasgow, 2000.
[45] T.J. Coutts, Proceedings of the 11th International Photovoltaics Science and Engineering Conference (PVSEC-11), Sapporo, Japan, September 20–24, 1999.